Study on Contribution of Trimethyl Guanosine Synthase Tgs1 to Heterochromatin Formation in Fission Yeast

（トリメチルグアノシン合成酵素 Tgs1 の分裂酵母ヘテロクロマチン形成での役割に関する研究）

Laboratory of Bioorganic Chemistry,

Graduate School of Chemical Sciences and Engineering,

Hokkaido University

Hiroki Yu

Index

1 General Introduction

1.1. Heterochromatin

One of the major goals of the life sciences is to understand how the genetic information written in DNA is maintained and expressed timely.

Only about 10% of the genes in eukaryotic cells are expressed, and most genes are repressed [1]. These phenomena have attracted attention recently as epigenetics, in which gene expression and cell phenotype change after cell division without changing the DNA sequence. Transcriptional repression via chromatin structure is one of the major mechanisms of this gene repression.

In eukaryotic cells, DNA wraps around an octamer histone protein every 146 bp to form a chromatin structure (Fig. 1-1). The N-terminus of the histone protein contains a region called the histone tail, which influences the chromatin structure through modifications such as acetylation, methylation, and phosphorylation[2]–[4]. Chromatin structure can be broadly classified into heterochromatin and euchromatin. Euchromatin, which has a loose chromatin structure, is characterized by the modification that the 9^{th} lysine is acetylated (K9Ac) and the 4^{th} lysine is methylated (K4me), and genes in this region are actively transcribed. Alternatively, heterochromatin is characterized by methylation on the 9^{th} lysine (K9me) and Heterochromatin Protein1 (HP1)/fission yeast homolog Swi6 binding by recognizing this modification, and gene transcription is suppressed. Also it has condensed structure and provides an environment that promotes the assembly of kinetochore during

mitosis at centromere, which is essential for the correct segregation of chromosomes (Fig.1-2)[5]–[8].

1.2. Heterochromatin formation mechanism

The mechanism by which the location of heterochromatin formation is still largely unknown. From research using fission yeast, which is a model organism in heterochromatin research found that there are some mechanisms of heterochromatin formation pathways and one is RNAi pathway [9]–[11]. In the fission yeast centromere region, heterochromatin is formed by the RNAi pathway. Two distinct repeat domains, outer repeat sequence (*otr*) and inner repeat sequence (*imr*), extend from the center of the centromere to the end of the chromosome. The outer repeat sequence contains two different repeat elements called *dg* and *dh*. *dg* stands for "*dogentai",* and the repeat sequence next to *dg* is named *dh* because the letter after "g" is "h"[12], [13].

The initiator of the RNAi pathway is double-stranded RNA. Initially, the repression of transcription initiated by double-stranded RNA was reported in plants. Subsequently, the Dicer homolog Dcr1, RdRP homolog Rdp1, and Argonaute homolog Ago1 were identified in fission yeast [14]–[16], and these genes were reported to be involved in heterochromatin formation.

In the process of RNAi-dependent heterochromatin formation in fission yeast, transcription occurs first at the centromere repeats, and the transcripts are converted into double-stranded RNA by RbRP, which is then converted into siRNA by Dcr1. One strand of siRNA is incorporated with the RITS complex

recruits the H3K9 methyltransferase Clr4 to methylate H3K9. The heterochromatin protein HP1, a fission yeast homolog of Swi6, recognizes H3K9me and binds to it. Swi6 binds to it and forms it as heterochromatin (Fig. 1-3). Genes incorporated into the region of heterochromatin are silenced, but not completely silenced. An interesting aspect of this mechanism is that the RNAi pathway forms an self-reinforcing loop of siRNA synthesis and heterochromatin formation, since disruption of any factor in the RNAi pathway results in the collapse of heterochromatin as well as loss of siRNA synthesis [17]. Furthermore, the repeated sequences of centromere heterochromatin are transcribed by Pol II, which is also plays an active role in siRNA synthesis [18], [19]. These findings suggest that RNAi pathway-related and heterochromatin-forming factors are localized in the vicinity of the centromere repeat sequence through the interaction among the factors and heterochromatic non-coding RNA, and that a series of heterochromatin-forming processes starting from transcription may be mutually reinforcing.

In vertebrates, heterochromatin is thought to be formed by a similar mechanism as in fission yeast. Knockout of the Dicer-encoding gene from chick DT40 cells or mouse ES cells results in abnormal heterochromatin formation in the centromeric region [20]. Many RNAs that do not encode genes (non-coding RNAs) are transcribed in higher eukaryotes, including vertebrates, and may contribute to heterochromatin formation. A well-known example of these noncoding RNA is the Xist transcript, which is involved in the inactivation of the X chromosome in mammals [21], [22]. Since the sex chromosomes of

mammalian cells are XY for males, XX for females, “X chromosome inactivation” that corrects the gene amount of the X chromosome occurs between males and females [21]. The Xist transcripts are thought to wrap around and accumulate on the X chromosome to recruit various epigenetic modifiers on chromatin to form heterochromatin.

1.3. Schizosaccharomyces Pombe as a model organism

Fission yeast has a heterochromatin structure in telomeres and centromeres like that of higher eukaryotes, such as humans, and RNAi factor homologous proteins are highly conserved (Table 1). Alternatively, unlike higher eukaryotes, RNAi factor genes have few redundant sequences [23]–[25], and thus the effects of gene disruption, including RNAi factors, can be analyzed. Thus, fission yeast has been widely used as a model organism in heterochromatin studies.

1.4. Trimethyl guanosine synthase 1

RNA methyltransferases play an important role in post-transcriptional maturation of most ribonucleic acids. All RNA methylation is post-transcriptionally induced by S-adenosyl-l-methionine (AdoMet)-dependent methyltransferases. One of these is trimethylguanosine synthase 1 (Tgs1), which catalyzes trimethylguanosine (TMG) cap modification [26], [27]. Tgs1 converts the monomethyl guanosine (MMG) caps of small nuclear RNA (snRNA) and small nuclear RNA (snoRNA) to TMG caps, which known as the only enzyme that catalyzes two consecutive methylation steps.

Nuclear Receptor Peroxisome Growth Factor Activation Receptor (PRIP) is involved

in transcriptional activation by nuclear receptor, and the Tgs1 human homolog PIMT/TGS1 in has been identified as the PRIP-interacting protein with methyltransferase domain (PIMT) [28]. In mammalian cells, PIMT/TGS1 has a large N-terminal insertion sequence with no reported functional domain compared to Tgs1 of the fission yeast *Schizosaccharomyces pombe* (Fig. 1-4). Interestingly, a shortened form that lacks the N-terminal side of TGS1 is also expressed in mammalian [29]. This shortened sequence seems to be very similar to the fission yeast Tgs1. Recently, crystal structure analysis revealed that the three-dimensional structure of the catalytic domain of Tgs1 is highly conserved among eukaryotes [30], [31] (Fig. 1-5). A three-dimensional structural model of fission yeast Tgs1 was created by homology modeling, and MMG cap binding pockets were predicted [32]. RNAs currently known to be the target of TMG cap modification are snRNA, which is essential for pre-mRNA splicing, the transcripts from the telomere region, and HIV-derived viral transcripts [33]–[36].

In mammalian, the newly transcribed snRNAs U1, U2, U4, and U5 are generally synthesized in the nucleus as premature precursors with an MMG cap at the 5'end. MMG cap modified RNA is modification dependently exported to the cytoplasm, where seven associations occur with the Sm protein [37]–[39]. Sm proteins bind to snRNA followed by TGS1 TMG cap modification. The motor neurons (SMN) associate with several proteins, such as Gemin2-6, to form a complex which related to the assembly and metabolism of snRNA protein complex (snRNPs). TMG cap modification is thought to occurs after the Sm protein and SMN complex binds to snRNA. The nuclear transport protein Snurportin1 (Snp1) recognize TMG cap modification and re-import snRNPs to the nucleus and become a mature snRNA (Fig. 1-6).

Yeast snRNAs U1, U2, U4, and U5 are also reported to have TMG cap modification and experiments using cells depleted of Sm proteins showed that TMG cap modification was also dependent on the Sm complex. Accompanying the nuclear re-import of snRNA, Sm proteins and SMN complex localize in both cytoplasm and nuclear [39], [40].

However, since yeast Tgs1 localized in the nucleus and the Snurportin 1 homolog has not been found, it is unclear whether snRNA is transported to the cytoplasm where TMG cap modification occurs. In *Drosophila melanogaster*, the deficiency of TMG cap modification due to Tgs1 deficiency reduced splicing efficiency and inhibited germ cell development, but not snRNA localization. These reports suggest that vertebrate cell TGS1 have a different snRNA-processing process [39], [41].

Telomere homeostasis is a major determinant of replication lifespan, cellular senescence, and tumor progression [42] Human telomeres are composed of short repetitive sequences at the ends of chromosomes that are blocked from the DNA repair mechanism by a special capping complex [43], [44]. TMG cap modification has been found at the 5'end of human telomerase transcript (hTR). Although the detailed molecular mechanism has not yet been elucidated, TGS1 disrupted cells showed increased telomerase activity and telomere elongation, which suggest that TMG cap modification of hTR by TGS1 suppresses of hTR expression and telomere elongation [35]. In contrast, it has been reported that telomere repeat sequences are shortened in Tgs1 depleted budding yeast and fission yeast [44], [45]. The reason for this difference between species is unknown.

Impaired TGS1 homolog activity caused insufficient pupation in *melanogaster* [46], and embryonic lethality in mice [47], though the mechanism is unclear.

1.5. This study

I used fission yeast, which is a model organism in heterochromatin research, to show that loss of Tgs1 leads to a variegated defect in heterochromatin. Some *tgs1* disrupted cells had reduced levels of H3K9me with impaired silencing, but heterochromatin was restored after several generations. My analyses showed that Tgs1 mainly contributes to *de novo* formation of heterochromatin, which be achieved through multiple mechanisms, including the recruitment of RNAi factors via spliceosome on heterochromatic ncRNA and retention heterochromatic ncRNA on chromatin. These results showed the novel function of RNA trimethylguanosine cap-modifying enzyme Tgs1 in the heterochromatin formation and provides insights into the communication between epigenetic regulation and RNA modification.

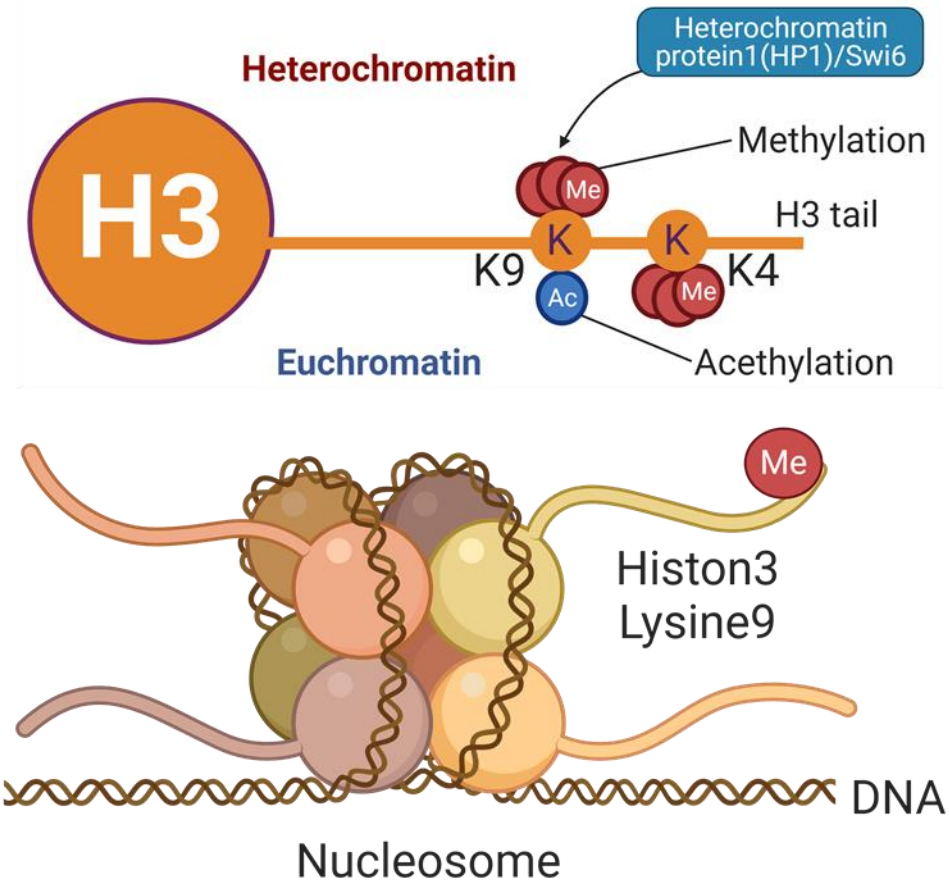

Fig.1-1 Model of Nucleosome

The histone protein forms a hetero octamer and 146 bp of DNA wraps around it to form a single nucleosome. There are multiple modification sites at the N-terminus of histone 3, and the 9th lysine undergoes methylation or acetylation modification.

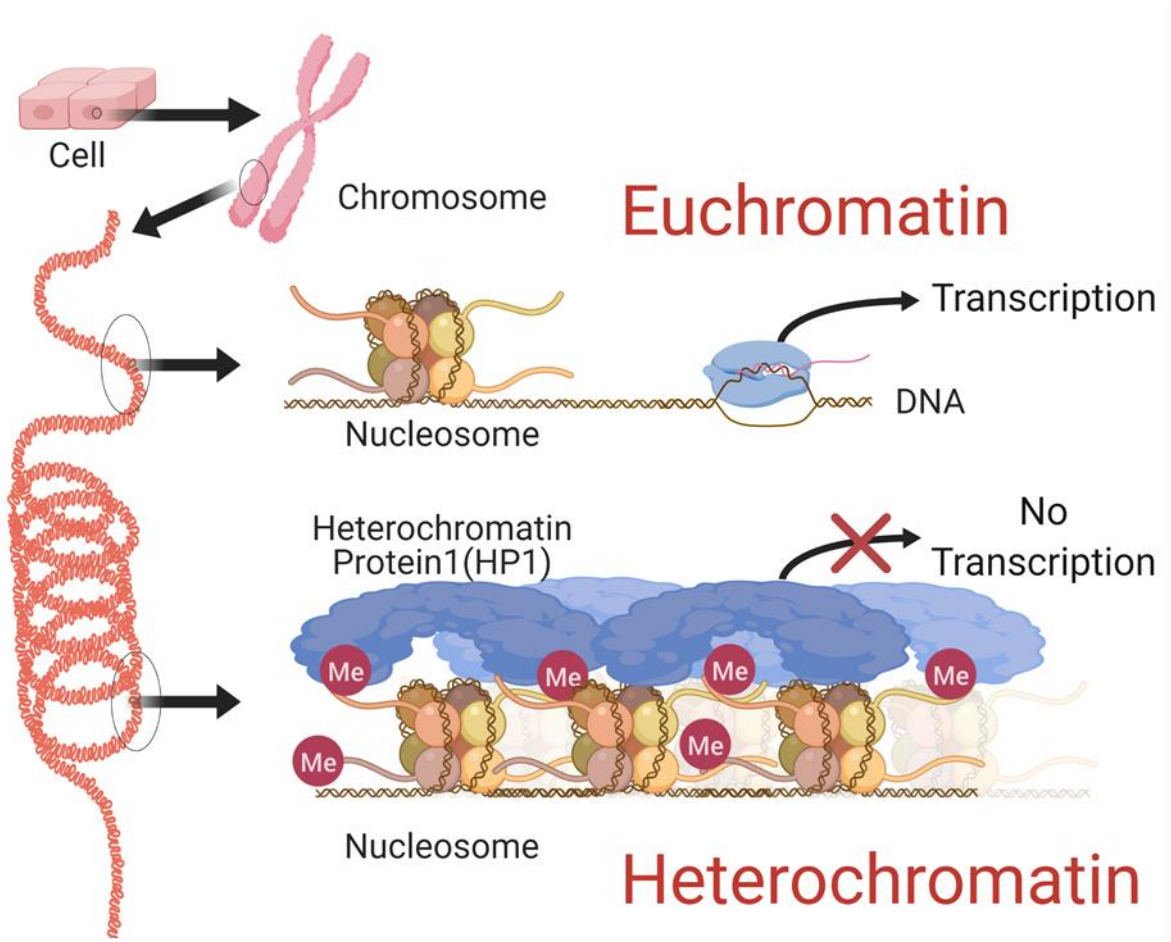

Fig.1-2 Model of two types of chromatin structure

Euchromatin is present in the region of active transcription.

Heterochromatin is formed in the centromere and telomere regions, and the genes contained in those regions are not transcribed.

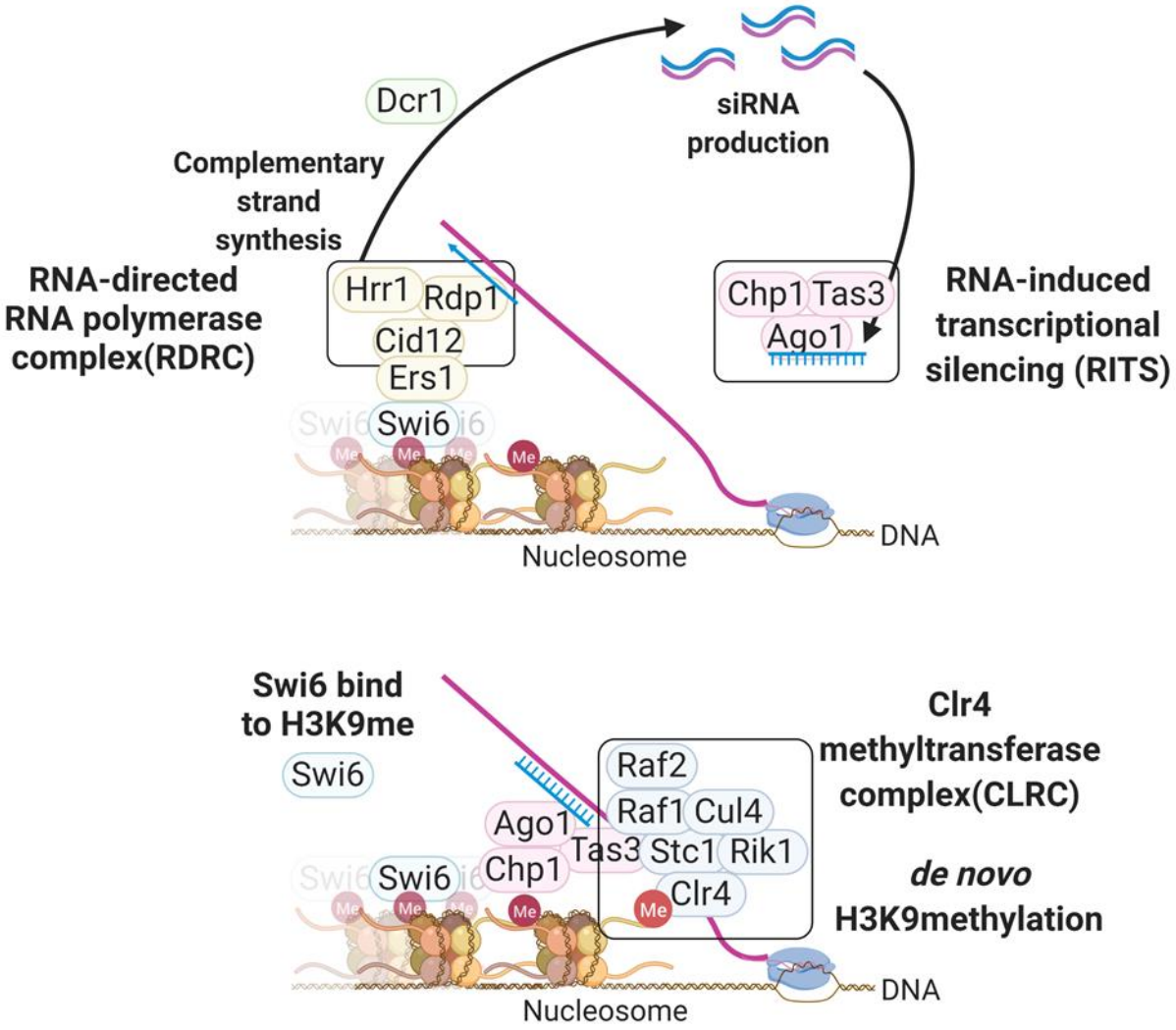

Fig.1-3 Schematic of Heterochromatin formation mechanism by RNAi pathway in fission yeast

After the transcript's complementary strand is synthesized by RDRC, it is converted to small RNA by Dcr1. Small RNAs are incorporated into Agol, a subunit of RITS complex. Through complementarity between siRNA and nascent RNA, the RITS complex binds to nascent transcripts to recruit CLRC containing the histone 3 lysine 9 methylase Clr4. Recognizing H3K9 methylated by Clr4, Swi6 binds to form heterochromatin.

Table1 Heterochromatin-forming factor homologs in various organisms

S. Pombe	***A.thaliana***	***C. elegans***	***M. Drosophila***	***H. Sapiens***
		heterochromatin assembly		
Dcr1	DCL1-4	Dcr1	Dcr1 Dcr2	DCR1
Ago1	AGO1-10	Rde1, Alg1-2	Ago1-3	AGO1-4
Rdp1	RDR1-6	Ego1, Rrf1-3	-	-
Hrr1	SGS2/SDE3	ZK1067.2	GH20028p	KIAA1404
Cid12	-	Rde3, Trf4	CG1126S	POLS
Rik1	DDB1	M18.5	Ddb1	DDB1
Cul4	CUL4	Cul4	Cul4	CUL4
Sir2	SIR2	Sir2-1	Sir2	SIRT1
Eri1	ERI1	Eri1	CG6393	THEX1
		Histon methylation, methylated histon binding		
Chp1	CMT3	-	-	-
Swi6	LHP1	Hpl1-2, F32E10.6	HP1	HP1α,β,γ
Clr4	SUVH2-6	-	Su(var)3-9	SUV39H1-2
		7-methylguanosine cap hypermethylation		
Tgs1	TGS1	TGS1	dTgs1	TGS1

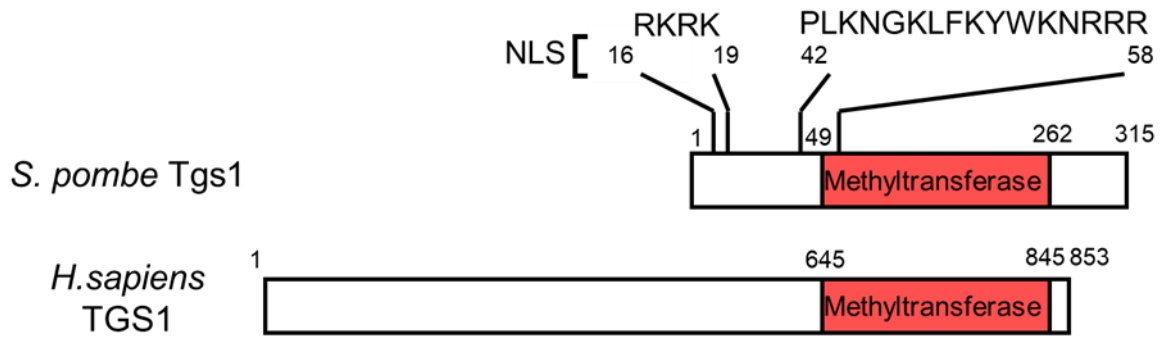

Fig.1-4 Comparison of protein secondary structures between fission yeast Tgs1 and human TGS1

The fission yeast Tgs1 and human TGS1 have highly conserved methylation transfer domains. On the other hand, human TGS1 has a huge insertion on the N-terminal side. No domains other than the methylation transfer domain have been found in any of the species.

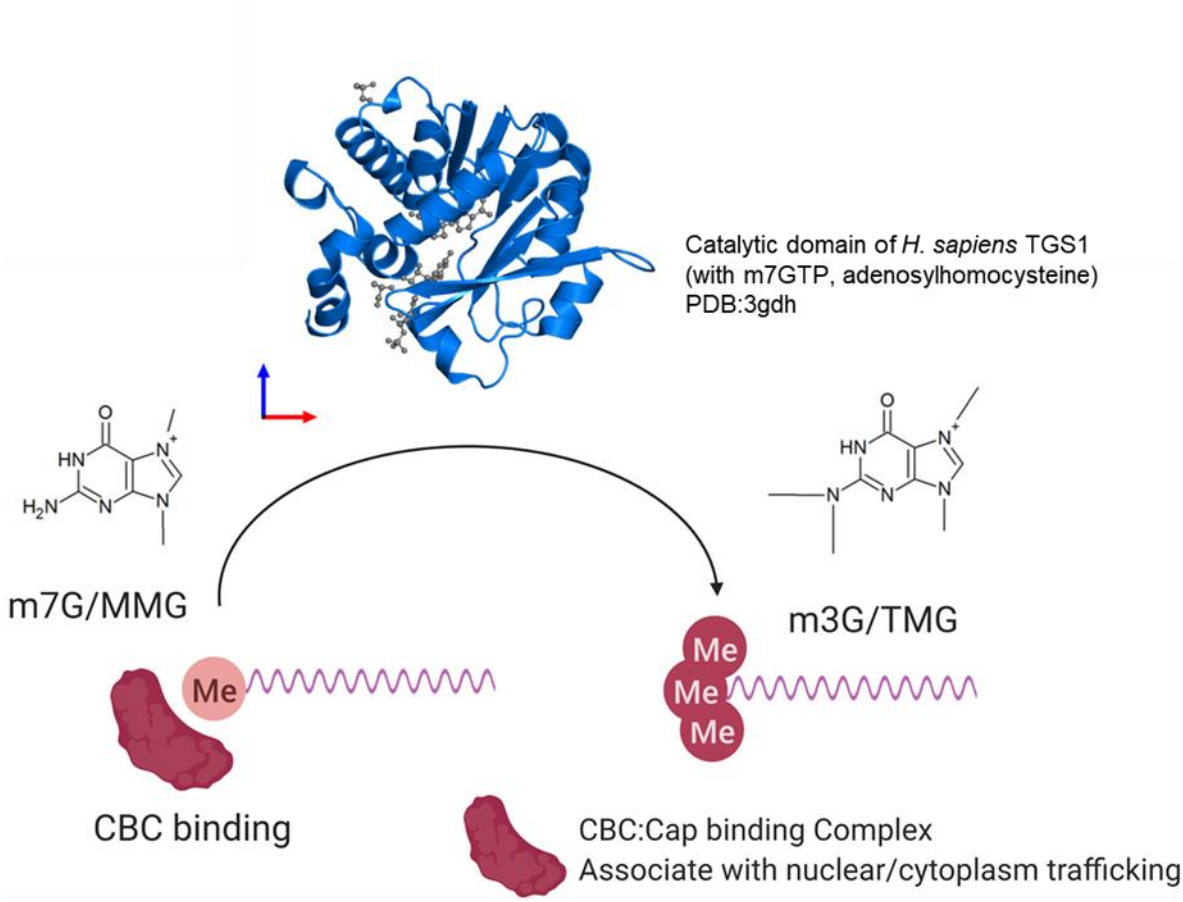

Fig. 1-5 TMG modification with Tgs1

Most mRNAs has monomethyl guanosine (MMG) cap. Tgs1 is the only currently reported enzyme that modifies MMG cap with a trimethylguanosine (TMG) cap. MMG-modified RNA binds to the cap-binding complex CBC, whereas TMG-modified RNA does not.

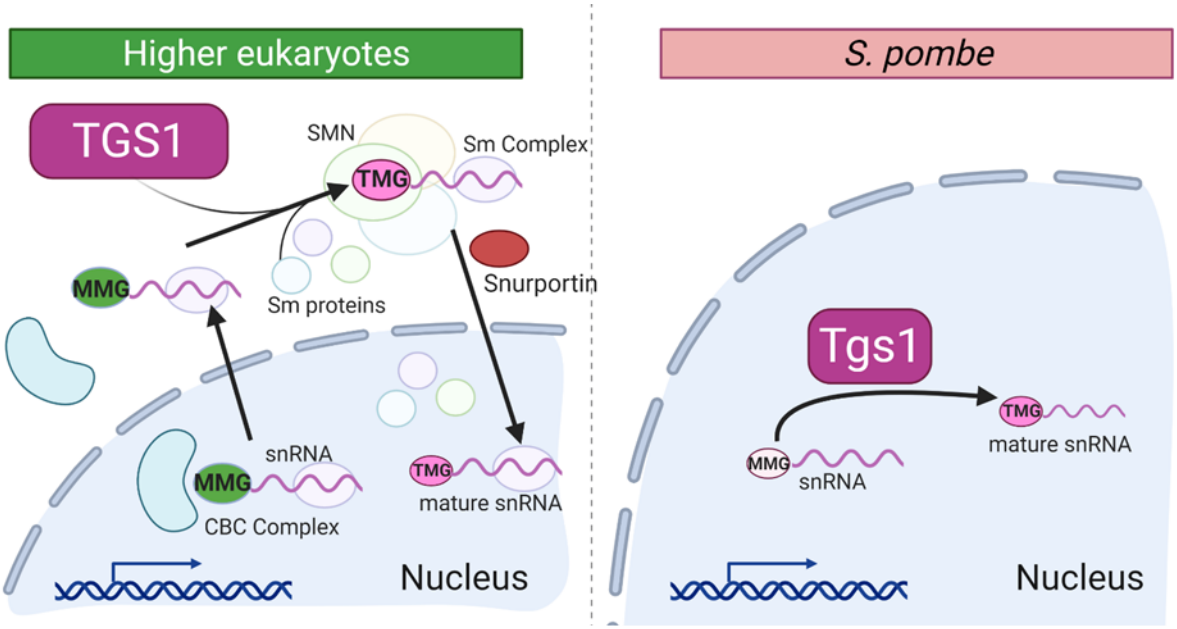

Fig. 1-6 Differences in TMG cap modification between higher eukaryotic cells and fission yeast

In higher eukaryotic cells, after transcription, the MMG-modified RNA molecule binds to the cap-binding complex and is transported to the cytoplasm. After binding of the Sm complex to the transported RNA, it is converted to TMG modification by TGS1 present in the cytoplasm. TMG-capped RNA is re-imported into the nucleus by Snurpotin1 (higher eukaryotic cells). On the other hand, because Snurportin 1 homologue has not been found in fission yeast, snRNAs get TMG cap modification in the nucleus without being transported to the cytoplasm (*S. pombe*).

2. Tgs1 deletion affect heterochromatin formation

2.1. Introduction

In fission yeast, most of the gene products involved in the formation and function of heterochromatin are localized in the spindle pole body (SPB) because centromeres, which contain large heterochromatin domains, clustered at SPB [48]. In a previous study of my laboratory, comprehensive database screening of genes whose products share characteristics with known heterochromatin-related factors identified several genes [49]. One of the genes whose deletion caused heterochromatin collapse phenotype was *tgs1*. Tgs1 is an RNA modifying enzyme that is highly conserved among many species, but its contribution or involvement in heterochromatin formation has not been reported.

As shown in Fig. 2-1, the central domain of the centromere in fission yeast is flanked on both sides by large repeat sequences on both sides and heterochromatin is formed on these repeat sequences. I used the strains that have *ade6*$^+$ and *ura4*$^+$ genes inserted in the repeats used to study heterochromatic silencing in these domains [5], [50].

The *ura4*$^+$ gene is a commonly used selection marker and is required for the synthesis of uracil; in the absence of the *ura4*$^+$ gene product, uracil is essential for growth. However, in a medium containing 5-fluoroorotate (5-FOA), wild type cells carrying the *ura4*$^+$ gene cannot grow because they convert FOA into toxic metabolites, and only *ura4*$^+$ gene-deficient cells can grow in the presence of 5-FOA [51]. Therefore, by introducing the wild type *ura4*$^+$ gene into the centromeric region, I can measure the heterochromatic silencing state: FOA resistance of cells having *ura4*$^+$ marker gene in heterochromatin well correlated with the level of heterochromatic silencing. Similarly, the *ade6*$^+$ gene is a system used to detect silencing more directly by observing colony color changes (Fig 2-

1). In the biosynthetic pathway of adenine starting from Phosphoribosyl pyrophosphate (P-ribosyl-PP) to adenine, the ade6 gene product metabolizes P-Ribosylamino imidazole to P-Ribosylamino imidazole carboxylate. P-Ribosylamino imidazole is a red-colored pigment, and the ade6 gene deleted colony shows red because P-Ribosylamino imidazole accumulates due to *ade6* gene disruption. Therefore, I can visualize heterochromatic silencing using cells harboring ade6^{+} gene inserted in heterochromatin: cells in which ade6^{+} is repressed by heterochromatin formed red colonies on low adenine plate while cells loos silencing of ade6^{+} formed white colony in the same condition.

2.2. Experimental procedure

2.2.1. Cell culture

The *S. Pombe* strains used in this study are listed (Table S1). Fission yeasts were cultivated in YES medium (yeast extract supplements: 0.5% (W/V), 3.0% glucose (W/V), 200 mg/L adenine, histidine, leucine, uracil and lysine hydrochloride) with shaking at 30°C, 180 rpm. Low adenine plates were used in the spot assay made by YES medium with 2% agar and without adenine. 5-FOA plates were used in the spot assay made by YES medium with 2% agar and 0.2% 5-FOA.

2.2.2. Colony Red/White ratio calculation

The cell number was measured by a particle size analyzer CDA-1000(Sysmex) according to the manufacturer's protocol. Five hundred cells were spread onto a 100 mm diameter containing low adenine media with agar. The cells were incubated at 30˚C for 4 days and photographed for the assessment. Each mutant was analyzed for 1000-1500 colonies. The software "OpenCFU" [52] was applied to the photographs of each mutant

and *clr4* disruptants. The redness was quantified by determining the RGB values and dividing the R value by the total RGB value; colonies that showed a value higher than the redness of *clr4* disrupted mutant were counted as “red colony”.

2.2.3. Serial dilution assay

Cells were cultured in YES medium to about 8.0×10^6 cells/ml, which is the logarithmic growth phase, and cell numbers were measured using CDA-1000 (Sysmex) according to the manufacturer’s protocol. Diluted series were prepared on 96-well plates with sterile water and spotted. Cells were incubated at 30°C for 3 days and photographed.

2.2.4. Primers

Primers used in this study were listed in Table S2.

2.2.5. qRT-PCR

Fission yeasts were cultured in 20 mL of YES medium to 1×10^7 cells/mL. The harvested cells were washed with PBS and stored at -80°C. Cells were crushed by freeze-thaw treatment consisting of rapid freezing in liquid nitrogen followed by vortexing and incubation in a water bath at 65 °C. This freezing-thawing treatment was repeated five times. After centrifugation, the cell pellet was suspended in 500 µl lysis buffer (50 mM HEPES pH 7.5, 140 mM NaCl, 1 mM EDTA pH 8.0, 0.1% TritonX-100, 0.1% sodium deoxycholate) and then the equivalent amount of acidic phenol was added to the suspension and heated at 65 °C for 1 hour. After the centrifugation, the aqueous phase was collected. RNA was precipitated by ethanol precipitation and treated with 5 U of recombinant DNase I (Takara Bio) at 37°C for 30 min. DNase I was removed by acid-phenol/chloroform treatment. Using the specific primers (Table S2), 1 µg of total RNA was reverse transcribed into cDNA by Prime Script Reverse Transcriptase (Takara Bio)

at 42°C for 45 min. Quantitative PCR (qPCR) was performed using SYBR Green I dye on the Thermal Cycler Dice Real Time System TP-850 (Takara Bio). Relative concentrations of cDNA based on the standard curve were divided by the concentration of *act1*$^{+}$ to determine the transcript levels relative to *act1*$^{+}$. Error bars represent the standard deviation of the mean of three independent experiments (n=3). Each experiment was performed independently from cell culture to qPCR.

2.2.6. Chromatin immunoprecipitation

Fission yeasts were grown to 1×10^7 cells/ml in 50 ml YES medium. After cell culture, formaldehyde (Nacalai Tesque) was added to the medium to a final concentration of 1%, and the sample was cross-linked by shaking at 30°C for 30 min. Glycine was added to the medium at a final concentration of 125 mM, and the reaction was quenched at room temperature for 30 min. The cells were collected by centrifugation at 3000 rpm for 3 min in a 50 ml conical tube. Subsequent operations were performed on ice. The pellets were washed with 1 ml PBS (phosphate-buffered saline: 137 mM NaCl, 8.1 mM Na_2HPO_4-$12H_2O$, 2.68 mM KCl, 1.47 mM KH_2PO_4), resuspended in 400 µl lysis buffer (50 mM HEPES pH 7.5, 140 mM NaCl, 1 mM EDTA, 2mM PMSF, 0.1% Triton X-100, 0.1% sodium deoxycholate, 2% Protease Inhibitor Cocktail immediately before use on use) and transferred to 2 ml tubes. Zirconia beads (MSE PRO) were added to the tubes, and the samples were disrupted in a bead shocker (Yasui Instrument) at 2700 rpm (30 cycles of 30 sec ON, 30 sec OFF). After the disruption, the cell suspension was collected, 1 ml lysis buffer was added, and chromatin fragmentation was performed by sonication using a sonicator (Diagenode) that had been cooled to 1–4°C. The supernatant was then centrifuged at 15,000 g for 10 min, and the supernatant was collected. anti-H3K9me

antibody was a gift from Dr. Takeshi Urano, Shimane University. anti-H3 antibody was obtained from Abcam. Dynabeads Pan mouse IgG was obtained from Thermo Fisher Scientific and washed with lysis buffer. anti-H3K9me antibody was combined with Dynabeads with 200 µg/ml BSA and incubated for 2 h at 4°C with rotation. Samples reacted with the antibody-conjugated Dynabeads for 2 h, and then washed three times with the lysis buffer and high-salt buffer (50 mM HEPES pH 7.5, 500 mM NaCl, 1 mM EDTA pH 8.0, 0.1% Triton X-100, 0.1% sodium deoxycholate). Subsequent operations were performed at room temperature. To degrade RNA, RNase A (Nacalai Tesque) was added at a final concentration of 0.1 mg in 1 ml TE. Then, the mixture was resuspended in the elution buffer (0.5% SDS, 0.5 mg/ml Protease K) and incubated at 37°C for 1 h. Reverse crosslinking was performed at 65°C overnight. DNA was purified by phenol–chloroform treatment and ethanol precipitation to yield qPCR template DNA. qPCR was amplified on a Thermal Cycler Dice (TaKaRa) and detected by SYBR. Three wells were measured for each sample, and three experiments were performed for each sample; errors were calculated as SEM.

2.3. Results

2.3.1. Loss of Tgs1 caused unstable silencing at heterochromatin

My laboratory has previously found some genes that affect heterochromatin formation by comprehensive screening described in 2.2-introduction [49]. One of the deletion mutants, *tgs1Δ* showed silencing defects of marker genes *imr1L::ura4*$^+$ and *otrR1::ade6*$^+$ which inserted into the centromeric heterochromatin (Fig. 2-1). Both marker genes are repressed by the heterochromatin, resulting in the formation of red colony on low-adenine plates (silencing of *ade6*$^+$) and the growth defect on 5-fluorotic acid (5-FOA) (silencing of *ura4*$^+$). The phenotype of *tgs1Δ* was different from that of other typical heterochromatin mutants including *clr4* that encodes the only reported H3K9-specific histone methyl transferase. *tgs1Δ* showed a mixture of red and white colonies while *clr4Δ* showed uniformly white colonies. To investigate silencing states of red and white clones of *tgs1Δ*, I performed spot assays using cells cultures starting from the red and white colonies (Fig. 2-2, 3). There was no significant difference of growth on non-selective medium between *wild type* and *tgs1Δ Red* and *tgs1Δ White* cells as reported before [53]. *tgs1Δ Red* cells showed 5-FOA resistance with the same level as that of the wild type, while *tgs1Δ White* cells showed moderate 5-FOA sensitivity, indicating that *imr::ura4*$^+$ gene was partially de-repressed, or some cells lost silencing in *tgs1Δ White* cells. On the low adenine plate, *tgs1Δ Red* cells formed red colonies and small portion (about 3-5%) of white colonies, while *tgs1Δ* w*hite* cells formed a mixture of red and white colonies. These results showed that the loss of Tgs1 caused unstable silencing at centromeric heterochromatin.

2.3.2. Desilencing occurred in tgs1 disrupted cells

I analyzed RNA levels in *tgs1Δ Red* cells and *White* cells by quantitative RT-PCR (qRT-PCR) (Fig. 2-4). Consistent with the silencing defects observed in the spot assay (Fig. 2-2), the expression level of *ade6*$^{+}$ mRNA was increased by about five-fold compared with wild type in *tgs1Δ White* cells, although the increased level was lower than *clr4Δ* which increased more than 60-fold compared with wild type because heterochromatin was completely removed in this mutant. Similarly, ncRNAs transcribed from the pericentromeric *dg* and *dh* repeats were also increased. In *tgs1Δ Red*, *ade6*$^{+}$ mRNA as well as ncRNAs from *d*g and *dh* were marginally increased.

2.3.3. Histon3 Lysine9 Methylation level were reduced in tgs1 disrupted cells

I examined the level of heterochromatin-specific histone modification H3K9me by chromatin immunoprecipitation (ChIP) assay (Fig. 2-5). *tgs1Δ Red* cells retained 60% levels of H3K9me compared to wild type at *otr::ade6*$^{+}$ and centromeric heterochromatin repeats. In contrast, *tgs1Δ White* cells showed only about 5% levels of H3K9me at these loci. Since white clones derived clones also contained some red cells, as shown in Fig. 2-2, 3, I supposed that the residual H3K9me in *tgs1Δ White* cells is due to red colonies appeared in white colony-derived clones and these red cells are considered to be re-silenced in the process of cell proliferation. These results suggest that a small number of cells stochastically loose heterochromatin structure in the absence of Tgs1, but the resulting euchromatic state is metastable and could return to heterochromatic state.

2.3.4. Functional catalytic domain of Tgs1 is required for stable silencing at centromeric heterochromatin.

The 153rd tryptophan (W153) of fission yeast Tgs1 is an invariant residue in the catalytic domain among eukaryotic cells (Fig. 2-6). In budding yeast, the replacement of W178, which corresponds to the fission yeast Tgs1 W153, to alanine caused loss of TMG cap of snRNAs and snoRNAs, showing the essentiality of this residue for the formation of TMG cap [33], [54]. Therefore, I analyzed the alanine substitution mutants Tgs1 W153 for silencing at centromeric heterochromatin (Fig. S1). Spot assay on a low adenine plate and qRT-PCR analysis of *ade6*$^{+}$ mRNA and centromeric heterochromatin repeat *dg* and *dh* ncRNA showed that the C-terminal myc tagged Tgs1 (*tgs1-myc*) did not affect heterochromatic silencing (Fig. 2-7, 8). *tgs1-W153A-myc White* cells showed variegated silencing defects like *tgs1Δ* and spot assay using Red and White isolates of *tgs1-W153A-myc* cells showed obvious silencing defect in White isolates similar to *tgs1Δ White* cells (Fig. 2-2, 7, 8). qRT-PCR analysis also showed similar silencing defects of *tgs1-W153A-myc White* (Fig. 2-9). These results indicate that the catalytic domain of Tgs1, is required for stable silencing mediated by centromeric heterochromatin.

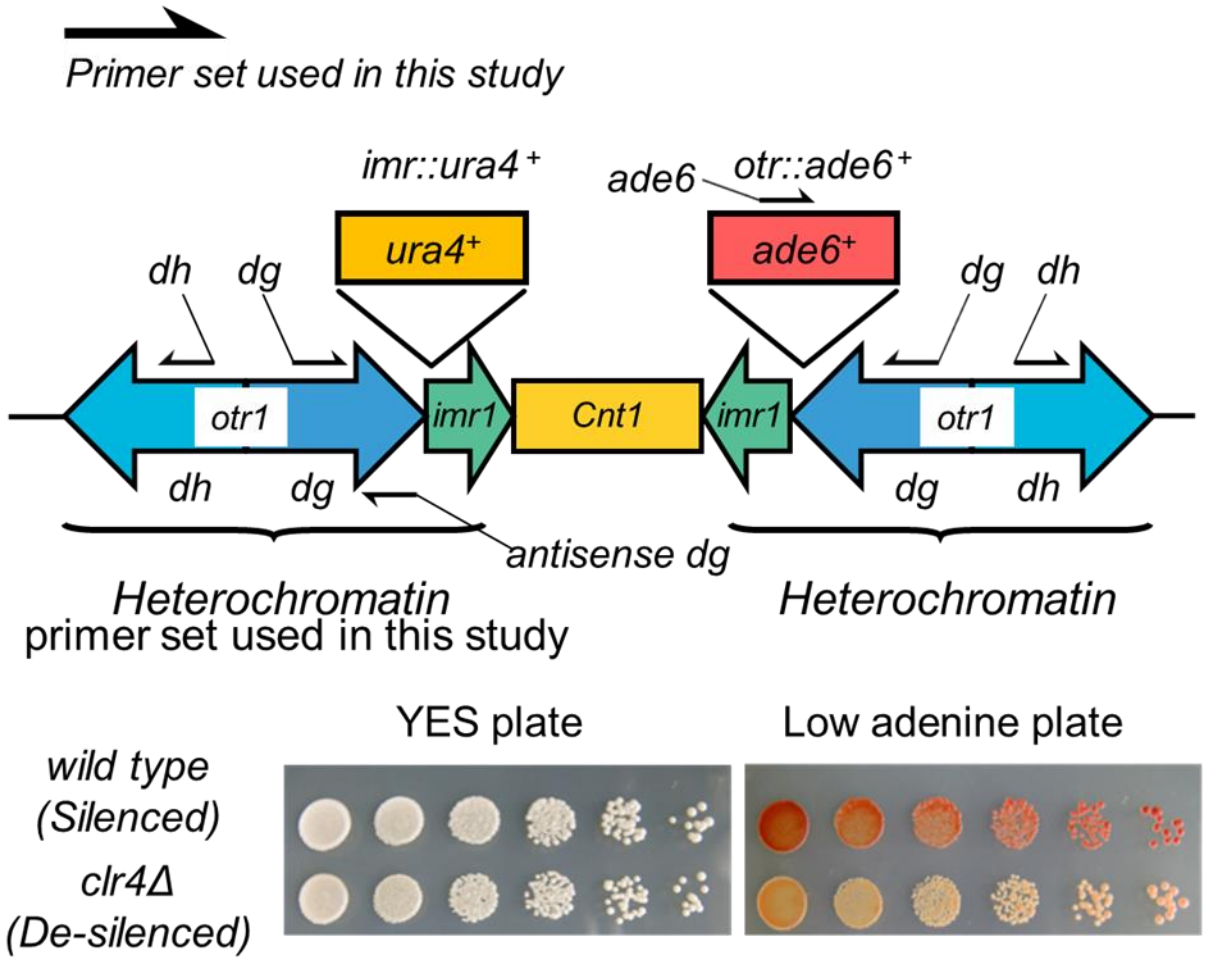

Fig. 2-1 Loss of Tgs1 causes disruption of heterochromatin

Schematic representation of the pericentromeric regions of the strains used in this study. *ura4*$^{+}$ and *ade6*$^{+}$ genes were inserted at the indicated position in the centromeric heterochromatin of chromosome 1. Black bars indicate the regions amplified by qRT-PCR, ChIP-qPCR, and RIP-qPCR.

When a cell line in which the *ade6*+ gene is introduced into the heterochromatin region is cultured on a low adenine plate, cells that do not express the adenine gene cannot metabolize the red pigment (Ribosylamino imidazole) and form red colonies. On the other hand, in the heterochromatin-disrupted strain, the ade6^{+} gene is expressed, so that a colony close to white is formed.

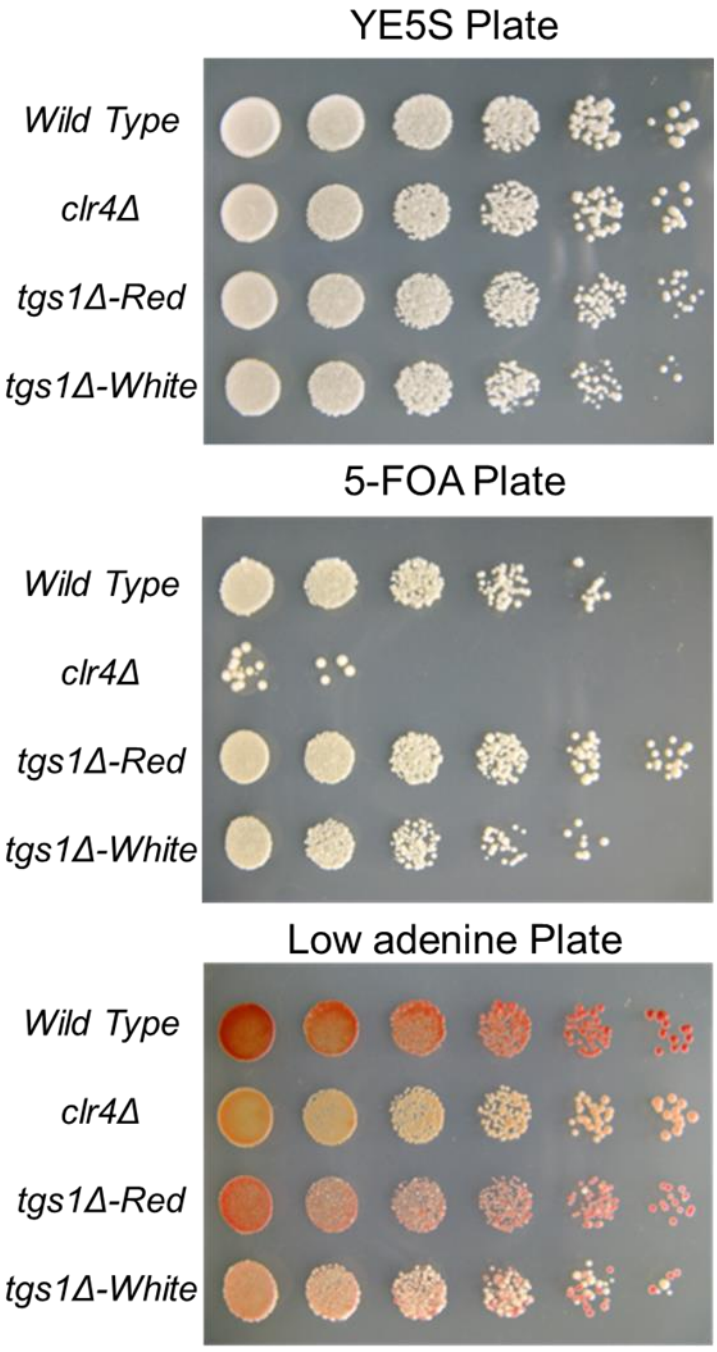

Fig. 2-2 Loss of Tgs1 causes disruption of heterochromatin

Silencing assay using the *imr::ura4*$^{+}$ and *otr::ade6*$^{+}$ reporter genes. Cells were spotted in 10-fold serial dilutions on YES plate with or with low adenine.

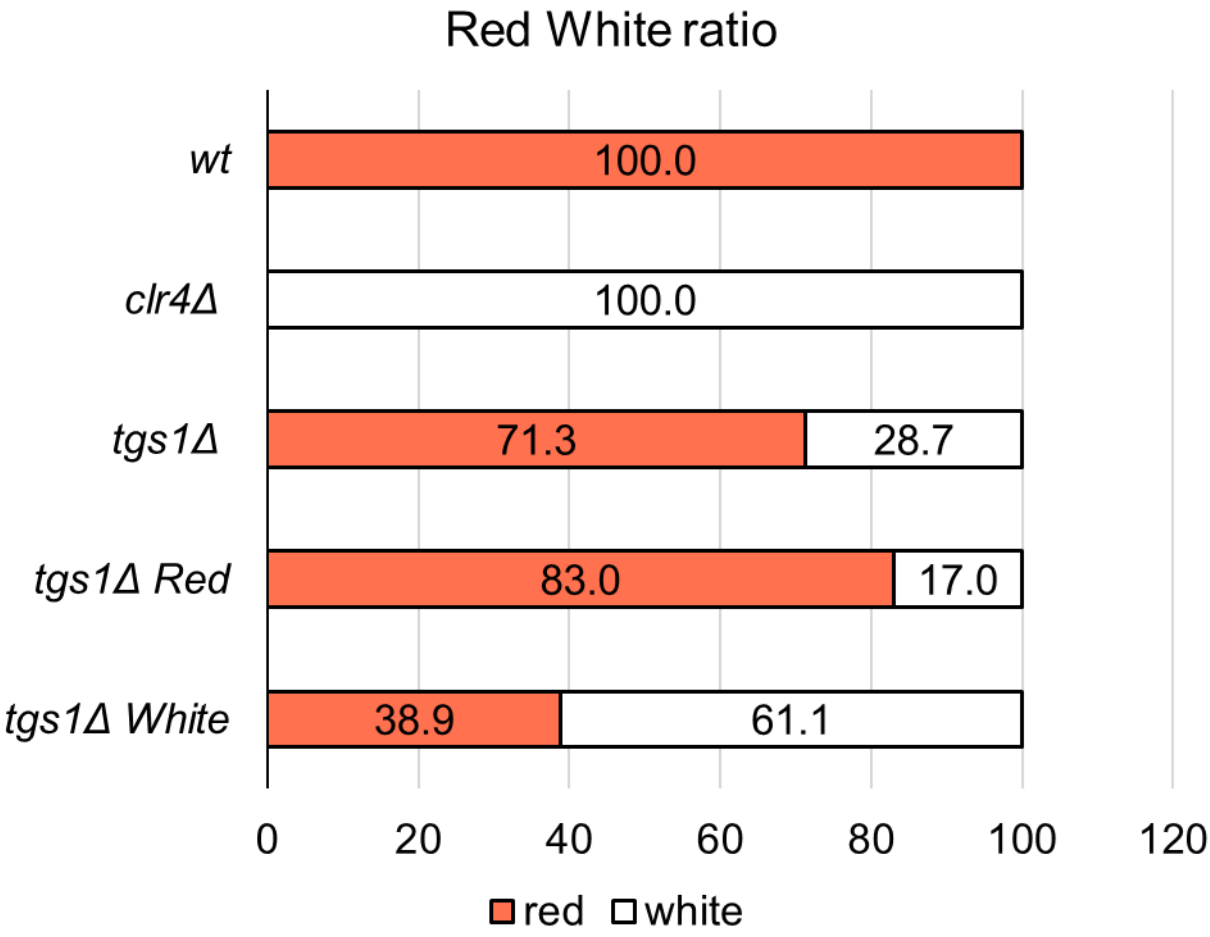

Fig. 2-3 Loss of Tgs1 causes disruption of heterochromatin

The proportion of red/white phenotypes in cells cultured on a low adenine plate was analyzed using OpenCFU as described in Methods.

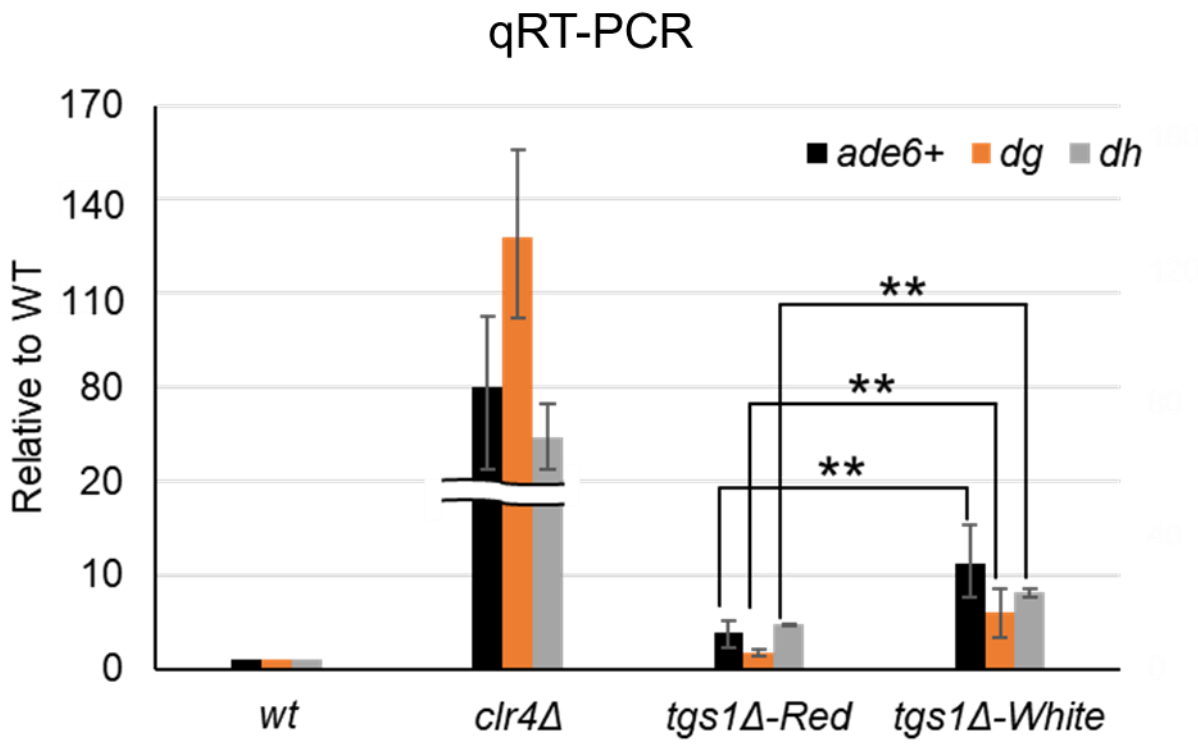

Fig. 2-4 Loss of Tgs1 causes disruption of heterochromatin

Quantitative Real-time PCR(qRT-PCR) of *otr::ade6*$^{+}$ and *dg, dh* transcripts relative to the *wild type*. cDNAs were synthesized using gene-specific reverse-strand primers. Primer pairs used for amplification were site-specific primers for *dg, dh*, and *otr::ade6*$^{+}$ at the peri centromere, and *act1*$^{+}$. qRT-PCR signals were normalized against *act1*$^{+}$ and are presented as fold change relative to the *wild type*, which was defined as 1. Error bars indicate SEM from three biologically independent experiments. *p < 0.05. p-values were determined using a two-tailed Student's t-test.

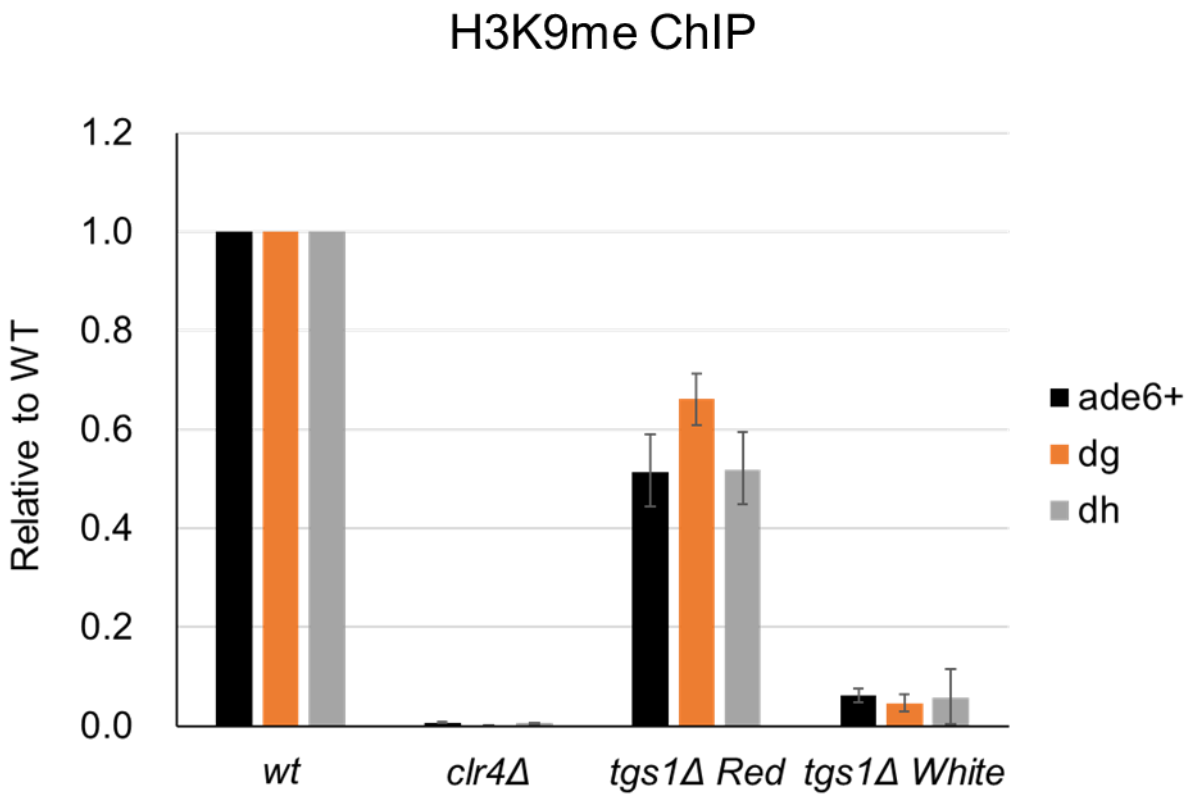

Fig. 2-5 Loss of Tgs1 causes disruption of heterochromatin

ChIP analysis of H3K9 methylation. Dimethylated H3K9 was immunoprecipitated, and the associated DNAs were quantified by qPCR using the same primer sets as in (Fig. 2-4). qPCR signals were normalized against the corresponding values in the wild type, which were defined as 1. Error bars indicate SEM from three biologically independent experiments.

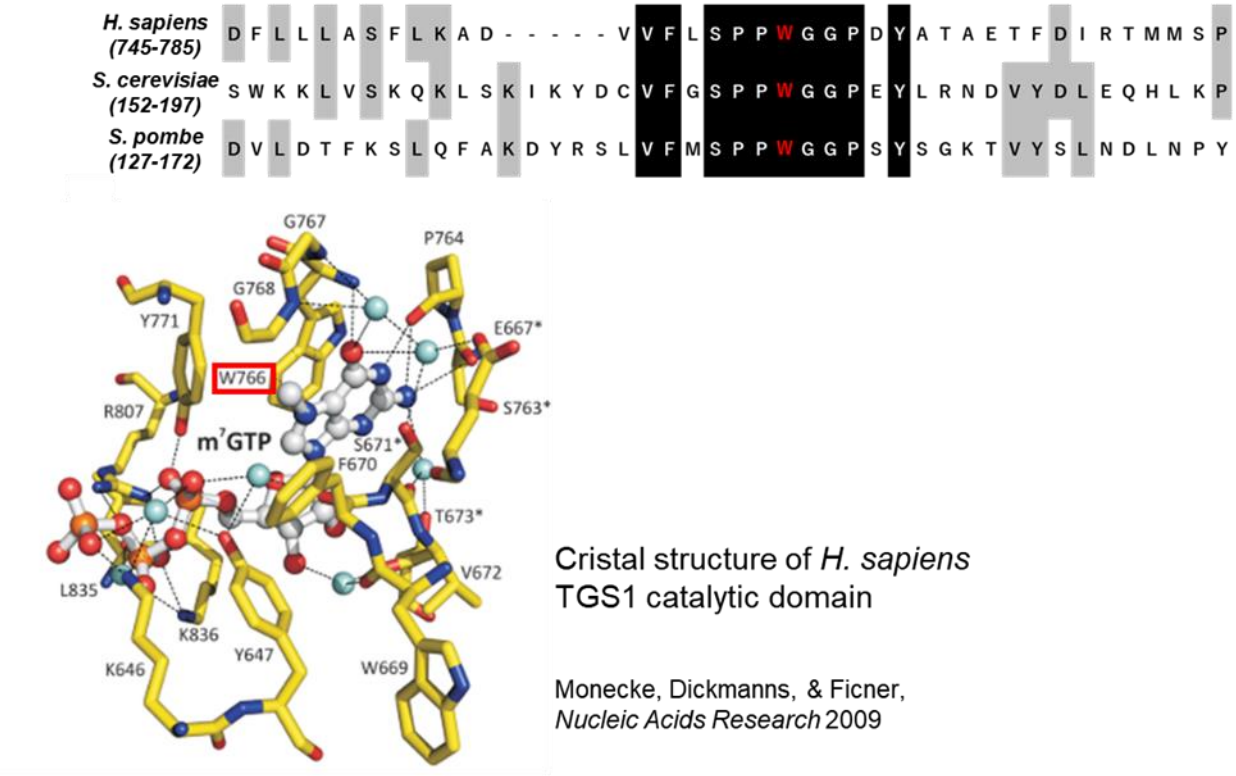

Fig. 2-6 Loss of Tgs1 causes disruption of heterochromatin

Schematic alignment of the amino acid sequences of the Tgs1 catalytic domain from *H. sapiens, S. cerevisiae,* and *S. pombe*. Identical and similar amino acids are highlighted in black and gray, respectively. The position of the W153A mutation in fission yeast Tgs1 is shown in red.

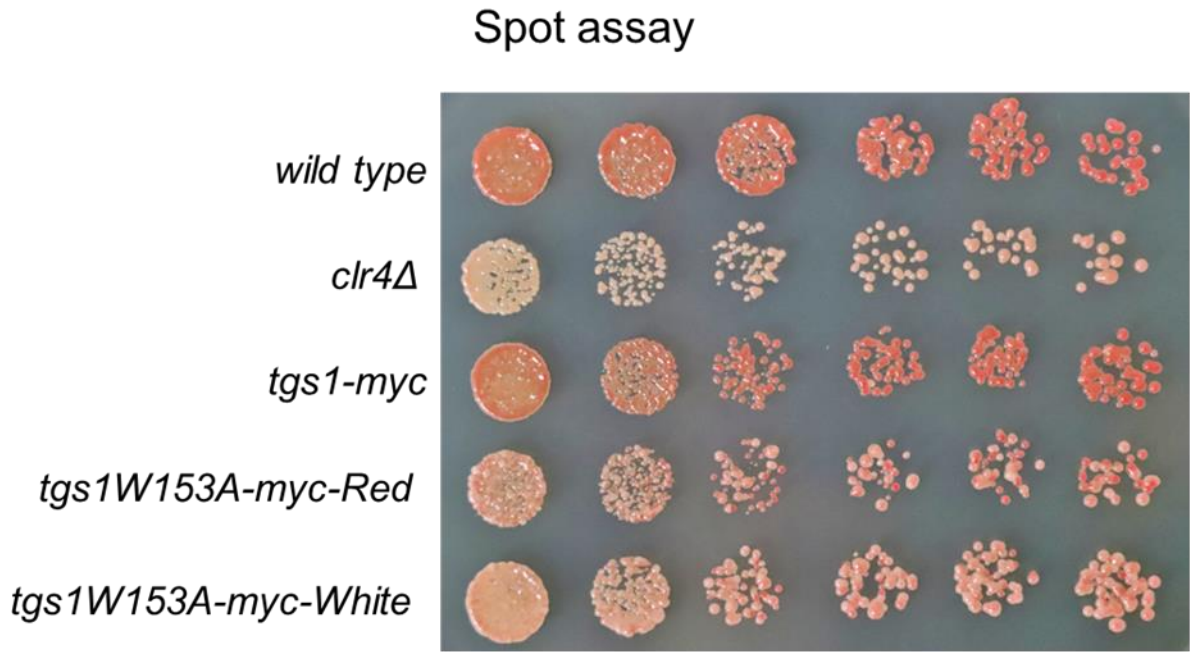

Fig. 2-7 Loss of Tgs1 causes disruption of heterochromatin

Spot assay of the *ade6*$^{+}$ marker gene. Indicated cells were spotted in 5-fold serial dilution on low adenine plate.

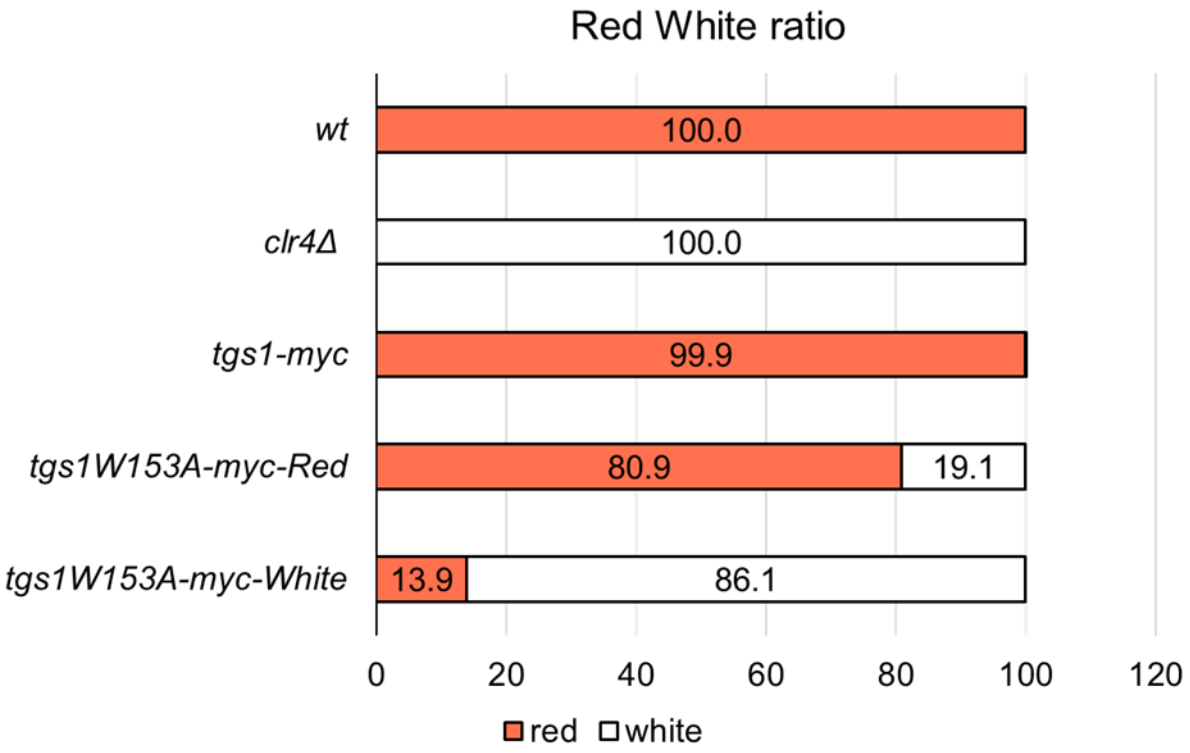

Fig. 2-8 Loss of Tgs1 causes disruption of heterochromatin

The proportion of red-white phenotypes in cells cultured on a low adenine plate was analyzed using OpenCFU.

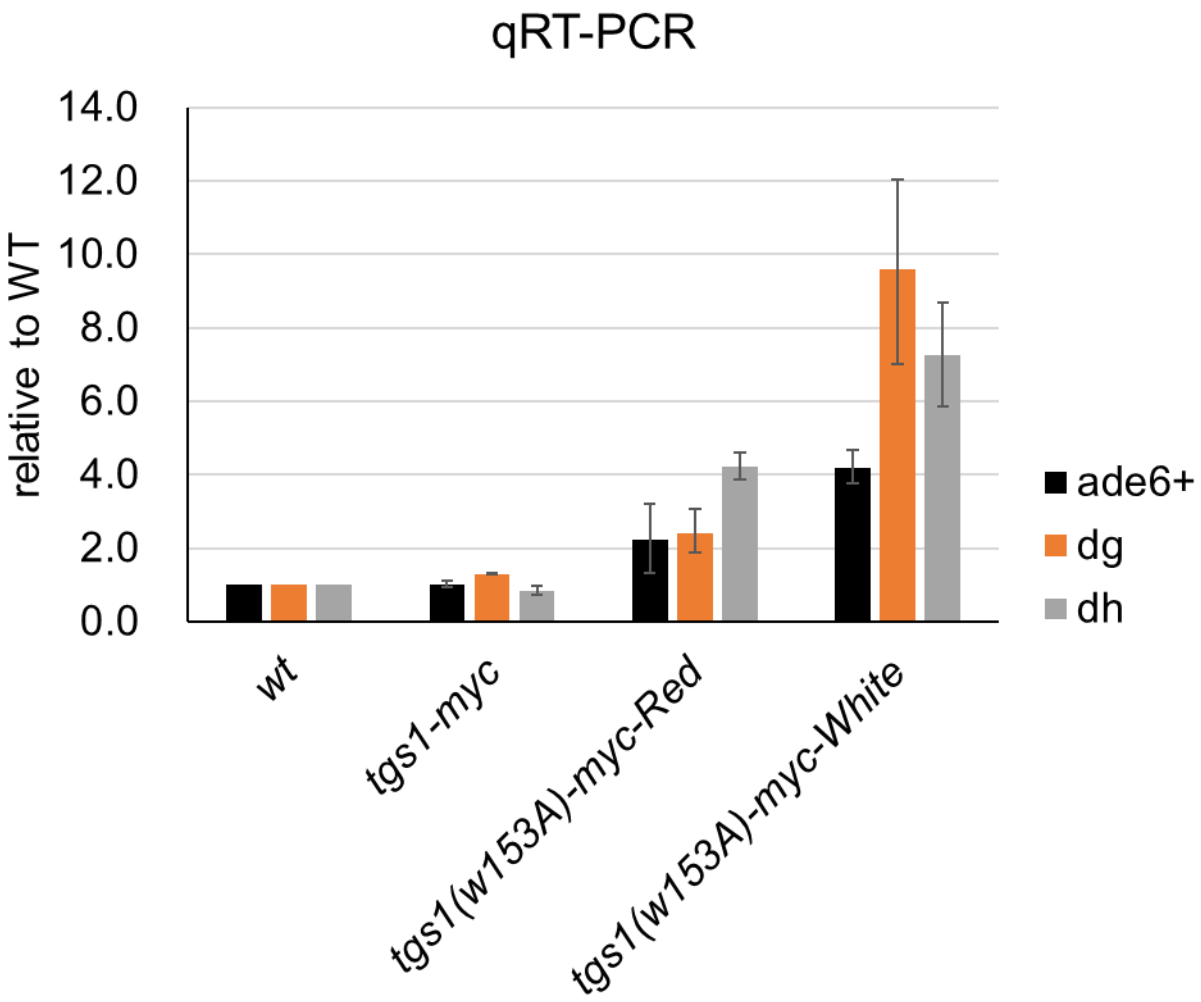

Fig. 2-9 Loss of Tgs1 causes disruption of heterochromatin

Real-time qPCR of *otr::ade6*$^{+}$ and *dg, dh* transcripts relative to the *wild type*. cDNAs were synthesized using gene-specific reverse-strand primers. Primer pairs used for qPCR were site-specific primers for *dg, dh*, *and otr::ade6*$^{+}$ at the peri centromere, and *act1*$^{+}$. qRT-PCR signals were normalized against *act1*$^{+}$ and are presented as fold change relative to the *wild type*, which was defined as 1. Error bars indicate SEM from three biologically independent experiments. *p < 0.05. p-values were determined using a two-tailed Student's t-test

3 Tgs1 is required for efficient establishment of heterochromatin.

3.1. Introduction

The previous results suggest that Tgs1 is an enzyme involved in heterochromatin formation. Next, I investigated how Tgs1 is specifically involved in heterochromatin formation. In general, the formation of heterochromatin contains two steps: establishment and maintenance. For the maintenance of heterochromatin, self-reinforcing loop of RNAi-dependent heterochromatin formation plays an important role: RNAi factors produce siRNA and deposit H3K9me, while Swi6 binding to H3K9me is required for RNAi factors to produce siRNA. On the other hand, for the establishment of heterochromatin from the euchromatin state where transcription is actively taking place, the RNAi pathway must be assembled in the absence of H3K9me and Swi6 to produce siRNA; some other factors play a role instead of Swi6.

To determine whether Tgs1 plays a role in heterochromatin establishment, I performed an *clr4-reintroduction* experiment, in which heterochromatin was completely disrupted by the deletion of H3K9methyltransferase *clr4* gene and then reconstructed by reintroducing the *clr4* gene. Using this system RNAi factors were shown to be absolutely required for heterochromatin establishment.

3.2. Experimental procedures

3.2.1. Transformation

Fission yeasts were cultured in 10 ml YES medium were collected and washed twice with 1 M sorbitol; all operations were conducted on the ice. The cells were resuspended

in 1 M sorbitol solution at 1.0×10^9 cells/ml, transferred to 100 µl cuvettes, and mixed with 2 µl transformation DNA. DNA was introduced using a Gene Pulser II (Bio-Rad, Hercules, CA, USA) at 2.25 kV/200 Ω/25 µF, and then cells were cultured in YES liquid medium for 1 h at 30℃ and then seeded on selective YES solid medium. The plasmid used to introduce the clr4 gene into the Clr4-deficient strain was kindly provided by Dr. Junichi Nakayama, RIKEN [55].

3.2.2. qRT-PCR, Chromatin immunoprecipitation

qRT-PCR and Chromatin immunoprecipitation were performed as previously described in 2.3. Primers used in this section are shown (Table S2).

3.3. Results

3.3.1. Tgs1 is involved in de novo establishment of heterochromatin

To analyze whether Tgs1 was involved in *de novo* heterochromatin establishment, I performed *clr4* deletion/reintroduction experiments [56] (Fig. 3-1). When the *clr4* gene was reintroduced to the *clr4Δ* cells harboring *ade6* marker gene in centromeric heterochromatin (Fig. 3-2; *clr4Δclr4(Re)*), all transformants formed red colonies on low adenine plate, which shows heterochromatic silencing was recovered. In contrast, when *clr4* gene was introduced into *tgs1 clr4* double disruptants (*tgs1Δclr4Δclr4 (Re)*), most colonies formed white colonies and only small on low adenine plates. Importantly, 17% of white colonies of *tgs1Δclr4Δclr4(Re)* cells produced red colonies indicating that *tgs1Δclr4Δclr4(Re)* cells can reestablish heterochromatin silencing with low efficiency (Fig. 3-3).

3.3.2. Silencing and H3K9methylation cannot recover without Tgs1

I analyzed the expression level of *ade6* marker gene and centromeric noncoding transcripts (Fig. 3-4) in the cells obtained from clr4-reintroduction experiments. Consistent with the silencing defects observed in the spot assay (Fig. 3-2), the expression levels of *ade6* mRNA as well as ncRNAs from dg and dh repeats were increased in *clr4Δ* and *tgs1Δ clr4Δ*. Consistent with previous reports, *Δclr4Δclr4 (Re)* showed low expression levels as wild type, indicating that re-introduction of *clr4* gene could successfully establish heterochromatin. Interestingly, *tgs1Δclr4Δclr4 (Re)* showed high expression level similar to the *clr4Δ* or *tgs1Δclr4Δ* double mutant. This suggests that some cells could not re-silence ade6 marker gene or centromeric noncoding transcripts without *tgs1* even if *clr4* exist. Next, I examined the level of H3K9methylation level (Fig. 3-5, 6). Consistent with the results of qRT-PCR, *clr4Δclr4(Re)* showed high H3K9methylation level similar to wild type. In contrast, despite having the *clr4* gene*, tgs1Δclr4Δclr4 (Re)* a showed very low level of H3K9methylation similar to the *clr4Δ*.

As shown in the spot assay (Fig. 3-2), *tgs1Δclr4Δclr4 (Re)* cells produced a small number of red colonies (Fig. 3*). These Red cells recovered the level of H3K9me comparable to wild-type cells, indicating that heterochromatin can be re-established in the absence of Tgs1 with low efficiency. Altogether, clr4-reintroduction experiments indicate that Tgs1 is required for efficient establishment of heterochromatin.

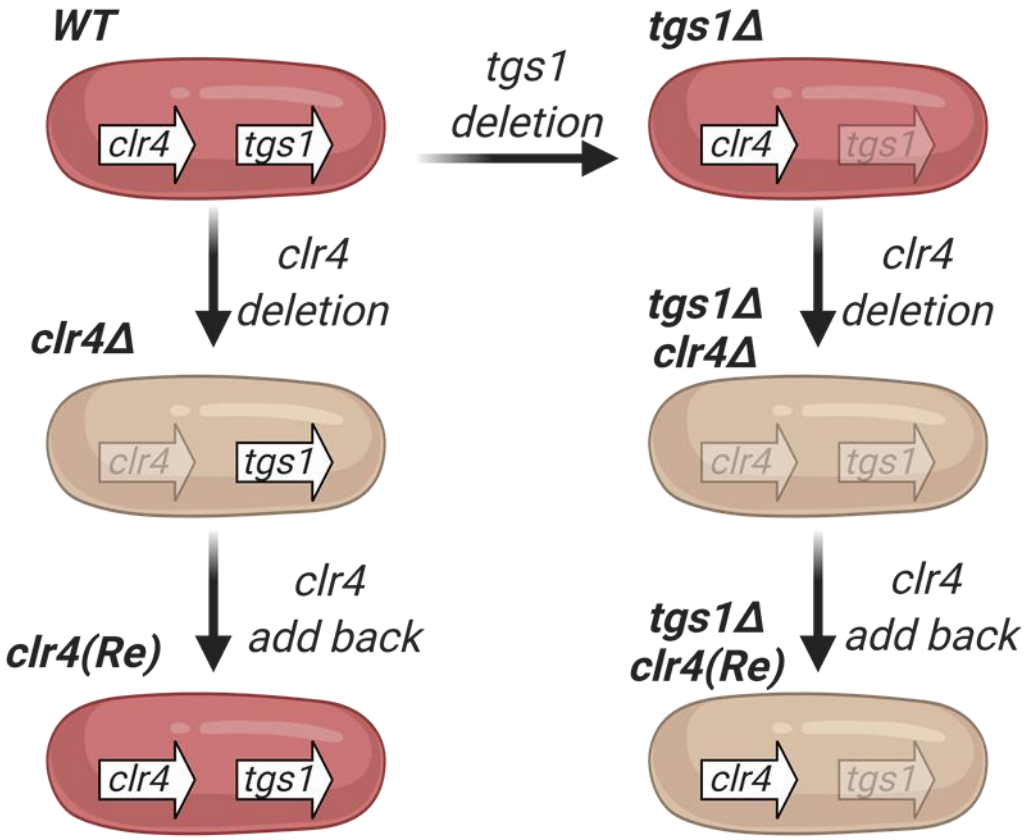

Fig. 3-1 Tgs1 is required for efficient establishment of centromeric heterochromatin

Schematic representation of the *clr4* deletion/reintroduction experiments. *clr4* was disrupted from the wild-type strain, and a strain into which the *clr4* gene was introduced again was prepared. In addition, *tgs1* and *clr4* were disrupted from the *wild type* to prepare a strain into which the *clr4* was re-introduced.

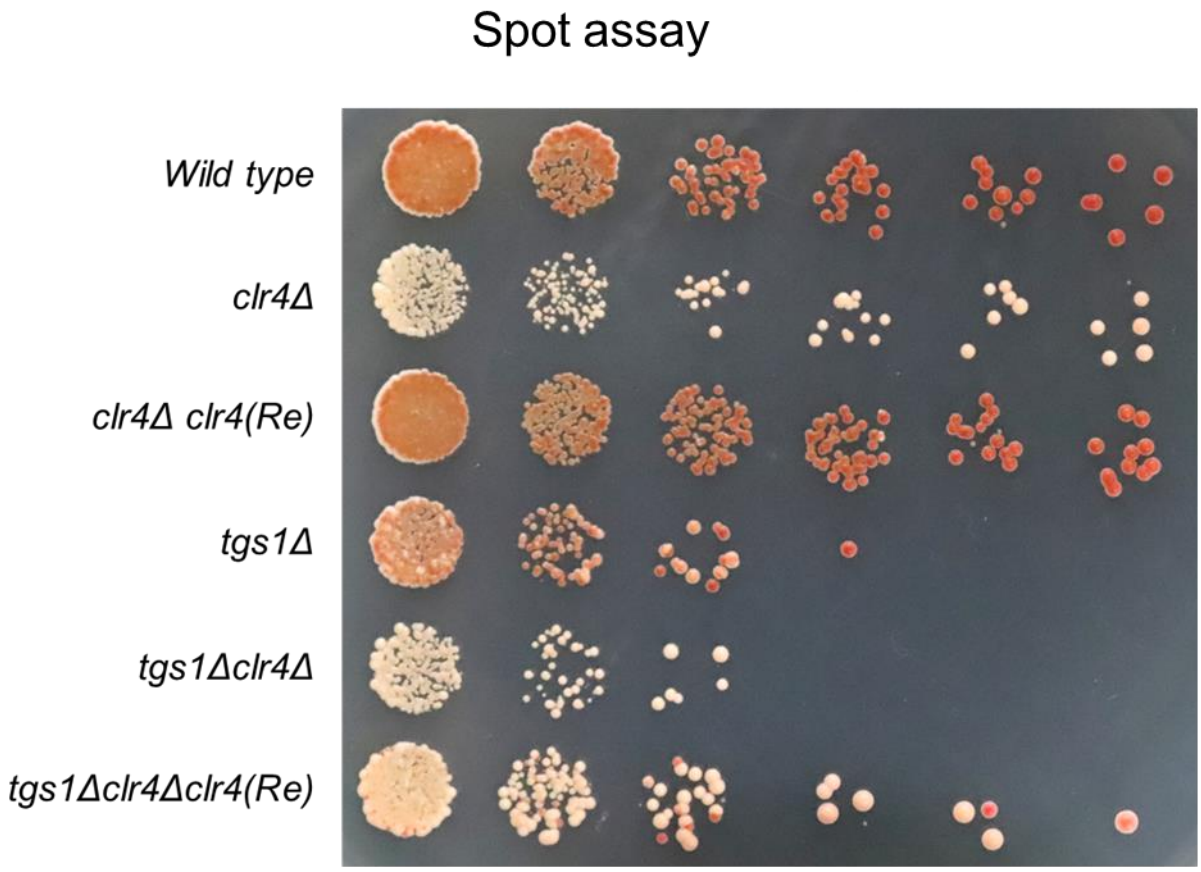

Fig. 3-2 Tgs1 is required for efficient establishment of centromeric heterochromatin

Spot assay of the *ade6+* marker gene. indicated cells were spotted in 5-fold serial dilution with low adenine.

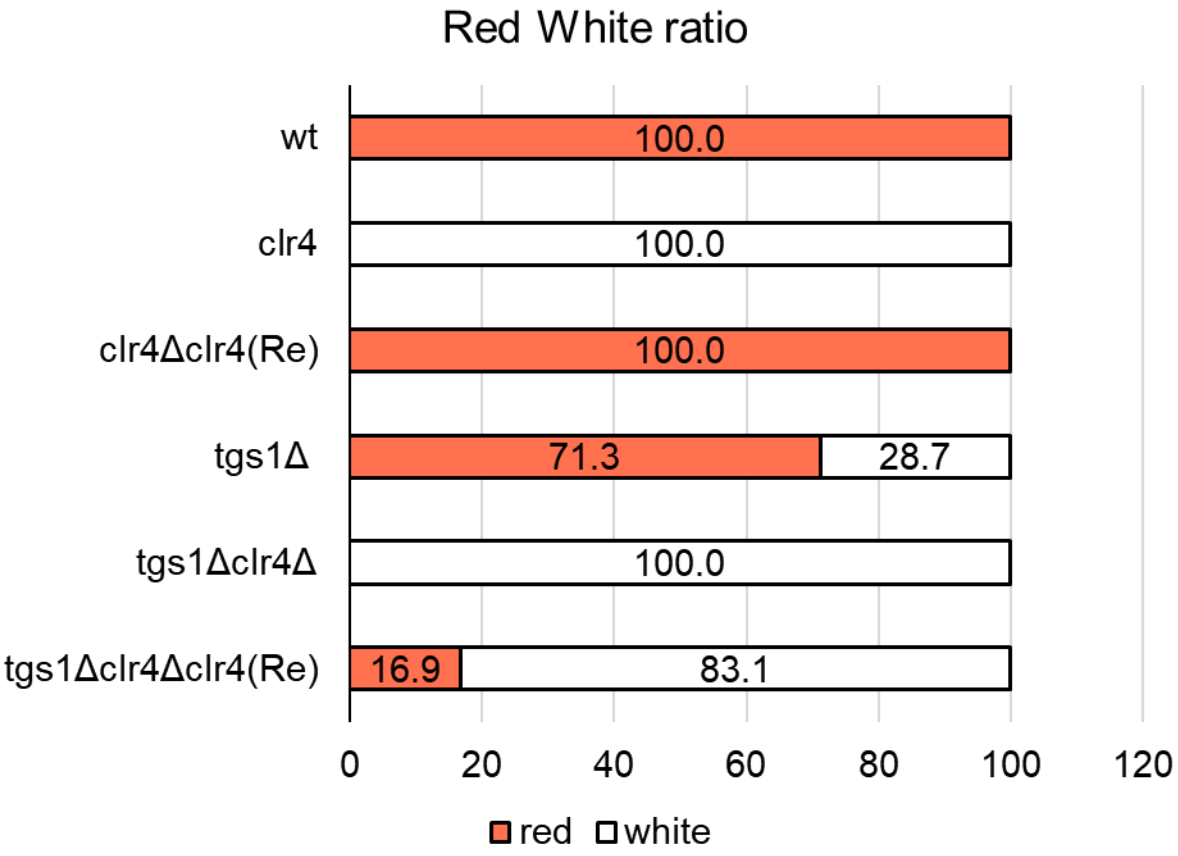

Fig. 3-3 Loss of Tgs1 causes disruption of heterochromatin

The proportion of red-white phenotypes in cells cultured on a low adenine plate was analyzed using OpenCFU.

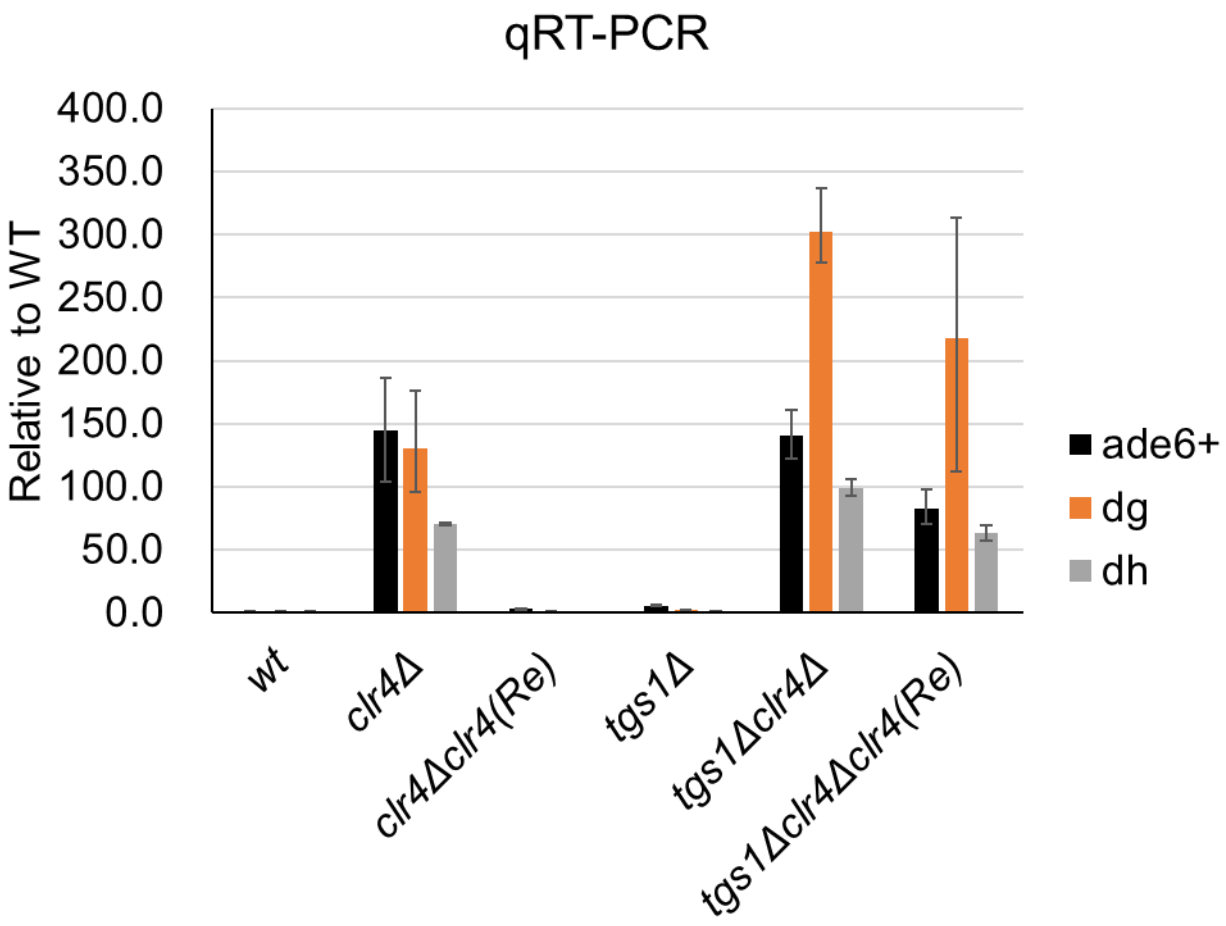

Fig. 3-4 Tgs1 is required for efficient establishment of centromeric heterochromatin

qRT-PCR of the *ade6*+ marker gene, centromeric repeat sequence *dg, dh* transcripts, relative to the *wild type*. cDNAs were synthesized by gene-specific reverse-strand primers. Primer pairs for qPCR were site-specific primers for *dg, dh,* and *otr::ade6*+ and *act1*+. qRT-PCR signals were normalized against the corresponding signals for *act1*+ and are presented as fold change relative to the *wild-type* value, which was defined as 1. Error bars indicate SEM from three biologically independent experiments.

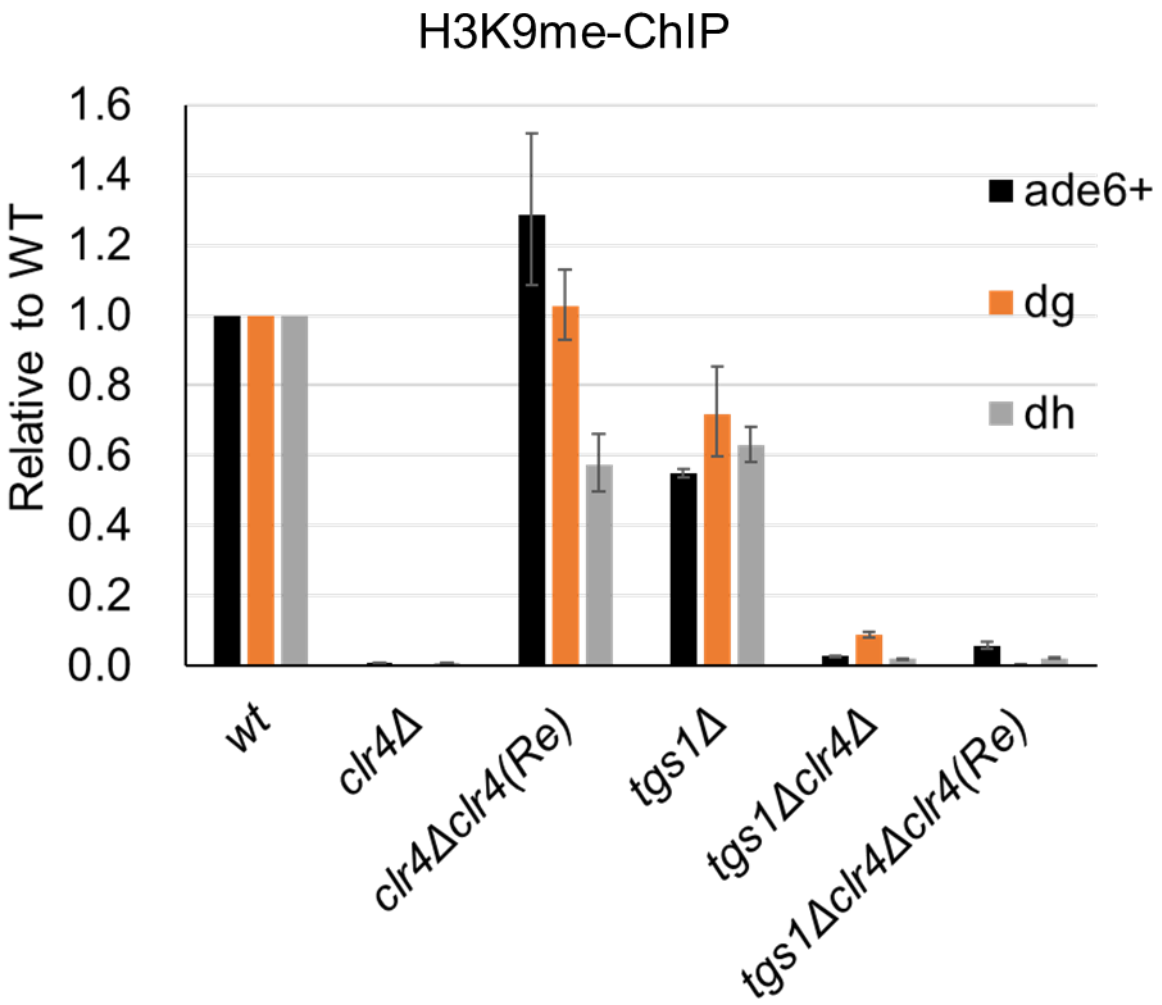

Fig. 3-5 Tgs1 is required for efficient establishment of centromeric heterochromatin

ChIP analysis of H3K9 methylation. Dimethylated H3K9 was immunoprecipitated, and the associated DNA was quantified by qPCR using the same primer sets as in (Fig. 3-4). qPCR signals were normalized against the corresponding values in the wild type, which were defined as 1. Error bars indicate SEM from three biologically independent experiment.

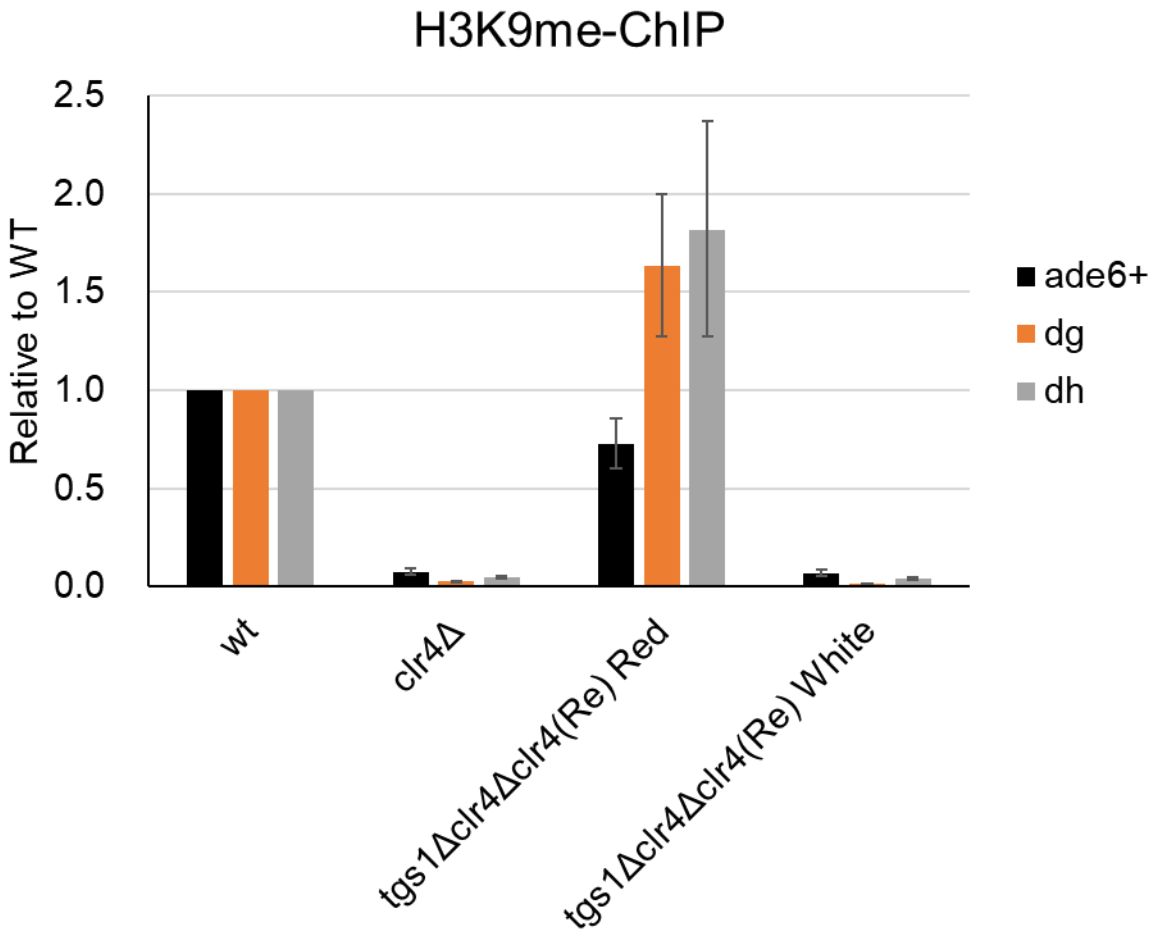

Fig. 3-6 Tgs1 is required for efficient establishment of centromeric heterochromatin

ChIP analysis of H3K9 methylation. Dimethylated H3K9 was immunoprecipitated, and the associated DNA was quantified by qPCR using the same primer sets as in (Fig. 3-4). qPCR signals were normalized against the corresponding values in the wild type, which were defined as 1. Error bars indicate SEM from three biologically independent experiment

4 Tgs1 functions in the Swi6-independent RNAi pathway

4.1. Introduction

Although RNAi-dependent heterochromatin formation plays a major role in centromeric heterochromatin, RNAi-independent heterochromatin also contributes centromeric heterochromatin [57]. Previous results of *clr4* deletion / re-introduction assays have shown that Tgs1 is involved in de novo formation of heterochromatin. In the initial stage of the establishment, the first siRNA should be produced in the absence of H3K9me and Swi6. Therefore, I hypothesized that Tgs1 is required for Swi6-independent heterochromatin siRNA formation.

4.2. Experimental procedure

4.2.1. Chromatin immunoprecipitation

Chromatin immunoprecipitation was performed as previously described in 2.3. Primers and probes used in this section are shown (Table S2).

4.2.2. Small interference RNA extraction

Small RNA was extracted by “mirVana miRNA isolation kit” (Thermo Fisher Scientific) according to the manufacturer’s protocol.

Cells for siRNA extraction were cultured in 100 ml/sample of YES medium, transferred to 50 ml conical tubes at 1 x 10^7 cells/ml and precipitated at 3200 rpm for 2 min and stored at -80°C. The cell pellet was washed with 1 ml of PBS, transferred to a 2 ml tube and centrifuged at 3200 rpm for 2 min and the supernatant was removed. One-third of the tube was filled with zirconia beads (MSE PRO), and 1 ml of Lysis buffer was added, and the cells were resuspended with 1 ml of lysis buffer. Cells were disrupted with

a Beads Shocker (Yasui Instrument) at 30 cycles, 60-seconds ON and 60-seconds OFF at 2700 pv and 0°C. 2 ml tubes were drilled and collected. The cells were set in a tube and the lysate was collected at 2000 rpm for 1 min. Tenth of the volume of miRNA homogenate additive was added to the lysate, vortexed for 2 minutes, and allowed to cool on ice for 10 minutes. An equal volume of acid phenol: chloroform was added to the cell lysate and vortexed for 1 min. The supernatant (aqueous layer) was collected in a new tube by centrifugation at 14,000 rpm for 5 min. One-third of the aqueous layer was added to 100% ethanol at room temperature and vortexed. The sample solution was placed on a column and centrifuged at 10,000 rpm 15 sec. To collects the sample that was not bound to the column. Two-thirds of the collected sample were added to 100% room temperature ethanol and vortexed for 1 minute. The samples were placed on a new column and centrifuged at 10,000 rpm for 15sec. The column was washed with 700 µl of miRNA Wash solution I at 10,000 rpm 15sec, 500 µl of miRNA Wash solution II was added and the column was washed in the same way. The column was again centrifuged at 10,000 rpm for 15 sec to dry the column, and 100 µl of elution solution, which had been previously heated to 95°C, was added to the column, left to stand still for 2 minutes, and then centrifuged at 10,000 rpm for 15 sec to collect siRNA. The concentration of siRNA was measured to be 700-1000 ng/µl.

4.2.3. siRNA detection

Small RNA was prepared as described above. DNA oligo probes corresponding to *dg* or snoRNA were used for 10 units of T4 polynucleotide kinase (Toyobo) The [γ32P] ATP was labeled at 3,000 Ci/mmol for 60 min at 37°C and purified using an Illustra Probe Quant G-50 microcolumn (GE Healthcare). Radioisotope-labeled oligoprobes were

hybridized at 42°C for 2 days and washed three times with 2× SSC (300mM NaCl, 30mM sodium citrate) containing 0.1% SDS. To detect *dg* or snoRNA signals, membranes were exposed to 4 days. Radioisotope signals were visualized on a BAS-300 (Fujifilm). Five hundred ng of siRNA was used for Northern blotting. Equal amounts of Gel-loading dye II (containing formamide) were added to siRNA loading samples and heated at 95°C for 3 min and then immediately quenched on ice. A Dynamarker pre-stain marker for small RNA plus (funakoshi) was used as a marker. For running, 15% sequence gel solution (1% glycerol, 1×TBE, 7M Urea) was used and the samples were run in 0.5×TBE buffer. Pre-run at 300 V for 5 min and then the urea in the wells were washed. Samples were loaded and swam at 300V 100min. The gels were washed with 0.25×TBE buffer and transferred using the Biorad semidry transfer system. three sheets of 3MM whattman filter paper thoroughly impregnated with 0.25×TBE buffer were laid on the electrodes, filter paper, membrane, gel, and filter paper in that order. The air was removed to prevent bubbles from entering. The electrode was set and transferred at 200mA for 60 min. The membranes were removed from the membrane and subjected to a UV-cross link (1200 μJ×100). After UV cross-linking, the ^{32}P labeled probes for detecting centromeric siRNA were produced by random priming of *dg* / *dh* repeats (Takara, Catalog No. 6045) was hybridized to the membrane overnight at 42 °C with the PerfectHyb Plus hybridization buffer (Sigma, Catalog No. H7033). The membrane was then washed with 2 x SSC 0.1% SDS buffer at 42 °C. The imaging plate was exposed to the membrane for 1 day. Oligonucleotide probes for snoRNA58 are ^{32}P-labeled at 5’ end by T4 polynucleotide kinase (Takara, cat # 2021A) were also hybridized to the membrane as a loading control.

The quantification was performed using ImageJ and normalized against the signal of snuR58 and presented as the fold relative to wild type, which defined 100.

4.3. Results

4.3.1. Tgs1 is required for Swi6-independent siRNA synthesis by RNAi

As described in the introduction, I speculated that Tgs1 is involved in the formation of Swi6-independent siRNAs, which could be required for heterochromatin establishment. To examine this hypothesis, I first analyzed H3K9 methylation in the absence of Swi6 by ChIP against H3K9me (Fig. 4-1). Single disruption strains of swi6 retained slightly reduced H3K9me levels compared to the wild type. In contrast, disruption of Dcr1, a component of RNAi and required for siRNA production, markedly reduced H3k9me levels. Similarly, H3K9me levels were markedly reduced in both tgs1 and swi6 disrupted with Dcr1.Interestingly, both *tgs1Δ* and *swi6Δ* showed significantly lower H3k9me levels similar to *dcr1Δ*.

Next, I analyzed the effect of tgs1 on the levels of siRNA in *swi6Δ* cells. I used probes complementary to siRNAs derived from centromeric repeat sequences to detect siRNAs. Disruption of Dcr1 resulted in loss of siRNA while disruption of *swi6* substantial level of siRNA was detected. The introduction of *dcr1Δ* into *swi6Δ* cells diminished siRNA, indicating that RNAi can produce siRNA in the absence of Swi6. Single disruption of *tgs1* marginally affected siRNA while siRNAs were disappeared in the double disruption of tgs1 and swi6 (Fig. 4-2, 3).

Although Tgs1 contributes little to siRNA synthesis in the presence of Swi6, it plays a major role in Swi6-independent siRNA synthesis. Together with the *clr4* deletion/ re-introduction assay (Fig. 3-1, 2), Tgs1 seems to play an important role in siRNA synthesis in the absence of Swi6 and it is required for efficient heterochromatin formation.

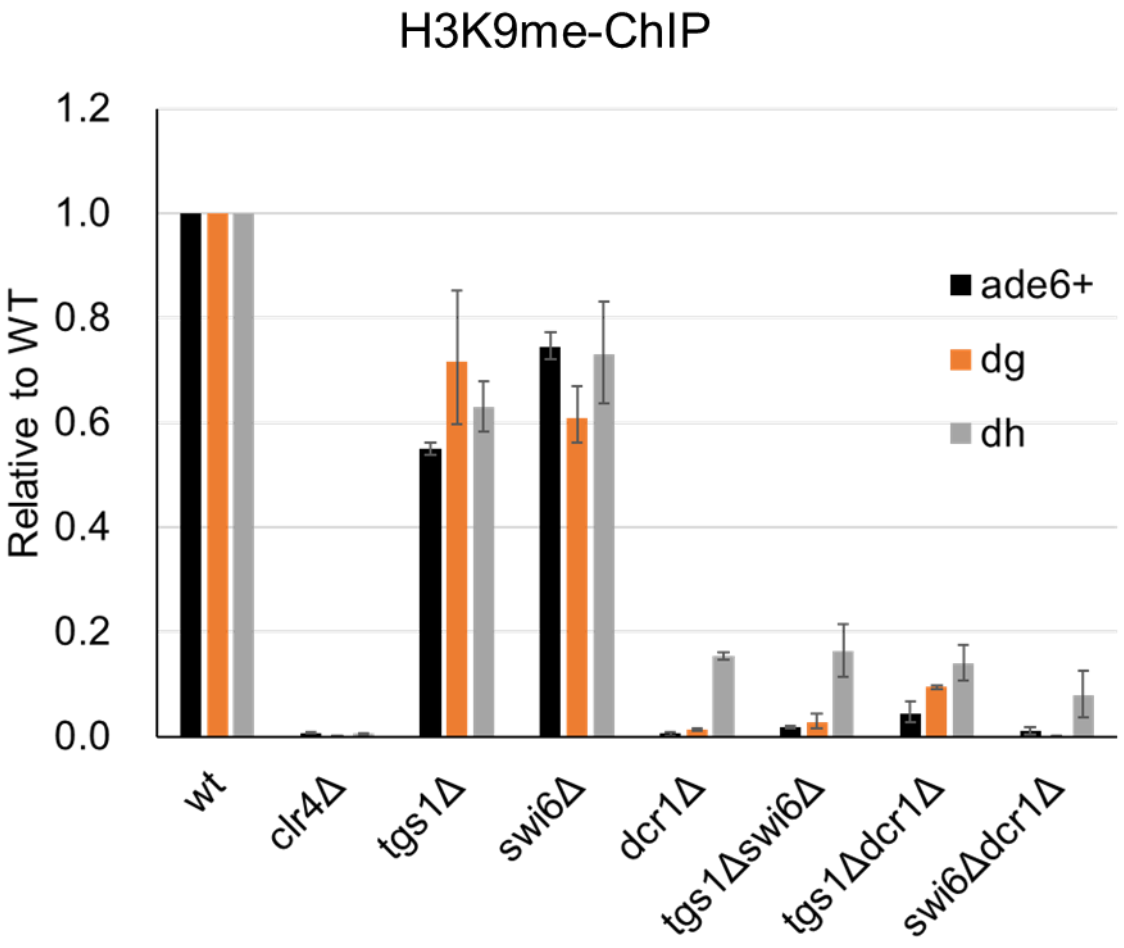

Fig. 4-1 Tgs1 functions in the Swi6-independent siRNA synthesis

ChIP analysis of H3K9 methylation in the indicated strains. Dimethylated H3K9 was immunoprecipitated, and the associated DNA was quantified by qPCR. Primer pairs for qPCR were site-specific primers for *dg, dh,* and *otr::ade6+* at the peri-centromere. qRT-PCR signals were normalized against the corresponding values in the *wild type*, which were defined as 1. Error bars indicate SEM from three biologically independent experiments

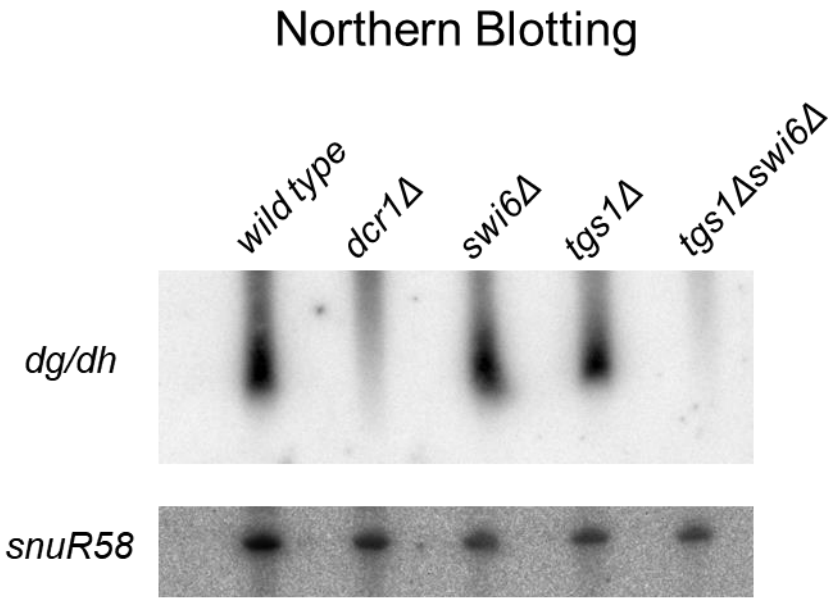

Fig. 4-2 Tgs1 functions in the Swi6-independent siRNA synthesis

Northern blot analysis of siRNA in the indicated strains. Small RNAs were selectively isolated by using the mirVana miRNA Isolation kit. *snuR58* was used as a loading control. Two biologically independent experiments were performed. Quantification of siRNA Northern blots shown in (Fig. 4-3).

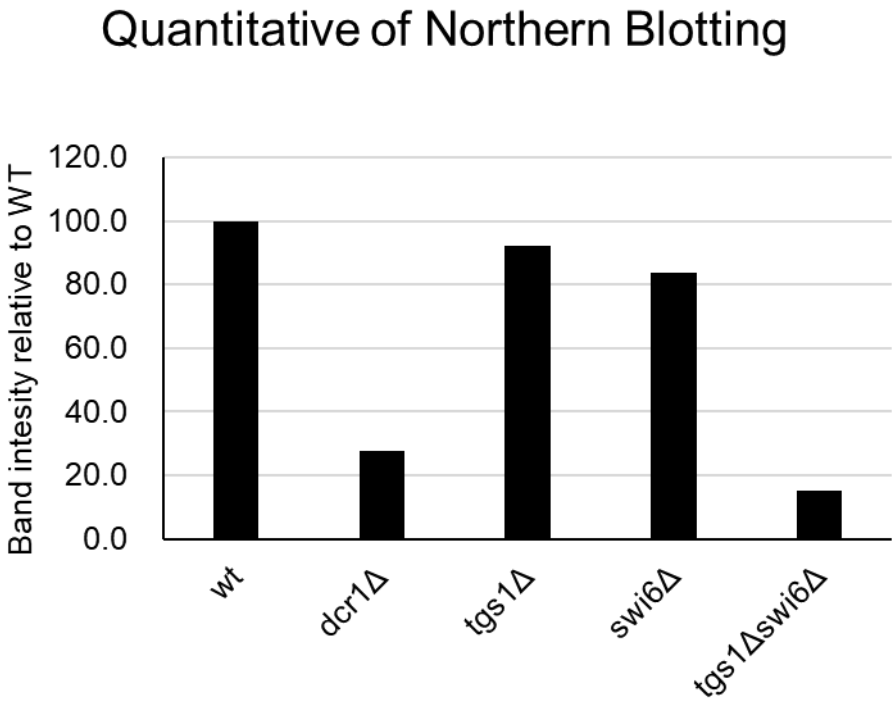

Fig. 4-3 Tgs1 functions in the Swi6-independent siRNA synthesis

Quantification was performed using ImageJ. Values were normalized against the corresponding *snuR58* signal and are presented as fold change relative to the *wild-type* value, which was defined as 100.

5 Loss of Tgs1 and/or Swi6 affects splicing efficiency of some introns of mRNA and heterochromatin noncoding RNA

5.1. Introduction

Small nuclear ribonucleoproteins are composed of small nucleic acid RNA (snRNA) and Sm proteins. The MMG caps of these snRNAs are hypermethylated by Tgs1 to produce TMG caps [29], [58]. Small nuclear ribonucleoproteins are components of the spliceosome, and loss of TMG in budding yeast causes defective splicing of a few introns in meiosis-specific genes, resulting in a sterile phenotype [59]. In addition, a recent study showed that TMG reduction in *melanogaster* impairs germline development by disrupting RNA processing, particularly of introns of smaller size or with weaker splice sites [60].

Interestingly, splicing factors also play positive roles in RNAi-dependent heterochromatin formation. Some splicing mutants, including *cwf10, prp10*, *prp16*, and U4 snRNA, decrease the level of H3K9me at centromeric heterochromatin, concomitant with a reduction in the level of siRNA [61]–[64]. A recent comprehensive RNA analysis of fission yeast has shown that some of these centromere heterochromatin-derived transcripts are predicted to have mRNA like introns named “cryptic intron” [62], [64], [65]. Intron of noncoding transcripts derived from centromeric repeats have very low splicing efficiency. So the spliceosome complex can stack on the transcripts to form a scaffold for binding of various factors via interaction [64]. Indeed, spliceosome associates with Cid12, a component of RDRC that plays an essential role in RNAi-dependent heterochromatin. Therefore, the spliceosome complex is thought to contribute to the formation of heterochromatin by the RNAi pathway. Consistent with this idea, the removal of the dg intron, mutation of the splice site, or replacement of the dg intron with

an euchromatic intron significantly reduces H3K9me levels. Based on the results of experiments with the shortened intron, the length of the intron is important but not the sequence [64].

These reported data raise the possibility that the loss of TMG-cap from snRNAs may cause improper formation of spliceosome on cryptic introns of hnc RNAs that prevent the recruitment of RNAi factors. Therefore, I decided to analyze the effects of loss of Tgs1 on splicing of heterochromatic non-coding RNA as well as euchromatic genes.

5.2. Experimental procedure

5.2.1. RNA immunoprecipitation for trimethyl guanosine cap

Total RNA was isolated by Ethanol precipitation as described in 2. 3.

20 µl of mouse Dynabeads were slurry resuspended in nuclease-free PBS, and then Anti-2,2,7-trimethylguanosine (m3G/TMG) mAb (MBL) was added. Beads and antibody were incubated overnight at 4 ℃. 40 µg of input total RNA and 500 µl of RNA-IP buffer (50mM Tris-HCl pH 7.5, 150mM NaCl, 1mM EDTA, 1% Triton X-100, 1.5mM DTT, 5U RNasin) were added to the tube containing antibody-conjugated beads, then incubated for 3 hours at 4℃.Beads were washed 4 times with 1 ml RNA-IP buffer. RNA was eluted from beads by adding 250 µl of 1% SDS/TE followed by incubation at 65℃ for 10minutes, and then 0.4 mg/ml Protease K at 37℃ for 30minutes. Immunoprecipitated RNA was extracted by acid phenol-chloroform followed by Ethanol precipitation. qRT-PCR was performed as described in 2.3. Primers used in this section are shown (Table S2).

5.2.2. Analysis of splicing efficiency by qRT-PCR

RNA was isolated as described in 2.3. Each gene was reverse transcribed with gene specific primer which showed in Table S2. The splicing defect was analyzed by electrophoresis through a 1.2% agar gel in TAE. The PCR products were visualized by ethidium bromide and quantified by scanning with a Molecular Imager Gel Doc XR$^+$ with Image LabTM software (BIORAD). Splicing efficiency was calculated by dividing the sum of the intensity of the spliced band and the unspliced band by the spliced band. Each band intensity was determined by Image LabTM software (BIORAD).

5.3. Results

5.3.1. Tgs1 is required for the trimethylation of U-snRNAs

First, I confirmed the requirement of Tgs1 for TMG cap of U1, U2 and U5-snRNAs by RNA-immunoprecipitation (RIP) assay using monoclonal antibody-specific for TMG cap (Fig. 5-1). Analysis of immunoprecipitated RNA by qRT-PCR showed that all snRNAs examined were precipitated by the TMG cap-specific antibody but *act1*$^+$ mRNA was not. In *tgs1Δ*, no snRNA was immunoprecipitated, showing Tgs1 really hypermethylated snRNA cap.

5.3.2. Loss of Tgs1 affects splicing efficiency of heterochromatic transcripts

To investigate whether the same reduction in splicing efficiency caused by tgs1 disruption as seen in other species, I analyzed the effect of loss of Tgs1 on splicing of the intron-containing RNAi factors, *ago1*$^+$ and *hrr1*$^+$ (Fig. 5-2, 3). I included *tbp1*$^+$ Which

encode TATA-binding protein as a control, because *tbp1*$^+$ had been used to detect the splicing defects in some splicing mutants [66].

Splicing efficiency of *ago1*$^+$ was decreased from 70% to 50% in *tgs1Δ* cells, whereas splicing of *hrr1*$^+$ was only marginally affected by the loss of Tgs1. Because siRNA production in *tgs1Δ* cells was comparable to that in *wild-type* cells (Fig. 4-2), the reduction in splicing of intron-containing mRNAs that encode RNAi factors is unlikely to affect siRNA synthesis. I also examined the effect of loss of Tgs1 on the splicing of mRNAs encoding RNAi factors in the absence of Swi6, as loss of Tgs1 decreased siRNA levels in this condition. Notably, the splicing efficiency of the *ago1*$^+$ intron was reduced in *swi6Δ* cells. As yet, I do not know the mechanism by which Swi6 affects splicing or the physiological meaning of its involvement. Loss of Tgs1 slightly decreased the splicing of *ago1*$^+$. By contrast, splicing of the *hrr1*$^+$ intron was hardly affected in *swi6Δ* or *tgs1Δswi6Δ* cells. As for *tbp1*$^+$, splicing efficiency decreased in *tgs1Δ* cells, whereas the loss of Swi6 caused a marginal reduction in *tbp1*$^+$ splicing. About 30% decrease was observed in *tgs1Δswi6Δ* cells. These results indicate that the loss of Tgs1 or Swi6 causes splicing defects in some genes including RNAi-related genes, suggesting that these defects are partly responsible for defects in siRNA synthesis in *swi6Δ* cells.

Next I analyzed the effect of the gene disruption on the splicing of cryptic introns of *dg*, *dh*, and *antisense dg* transcripts (Fig. S2).

In the wild type, the splicing efficiency of these cryptic introns was very low (less than 20%) as consistent (Fig. 5-4, 5) with a previous report [64]. Loss of Tgs1 did not cause a significant change in the splicing of these cryptic introns in the presence of Swi6. In the absence of Swi6, however, the splicing efficiency of *dg* intron decreased, whereas that of

antisense dg intron increased. Interestingly, double disruption of *tgs1* and *swi6* marginally affected the splicing of *dg* and increased the splicing efficiency of *antisense dg* but did not affect *dh* intron. These results indicate that the loss of Tgs1 affects splicing efficiency of heterochromatic non-coding RNAs, suggesting the loss of TMG cap from snRNAs caused a change of spliceosome formation on the cryptic introns on heterochromatic ncRNAs.

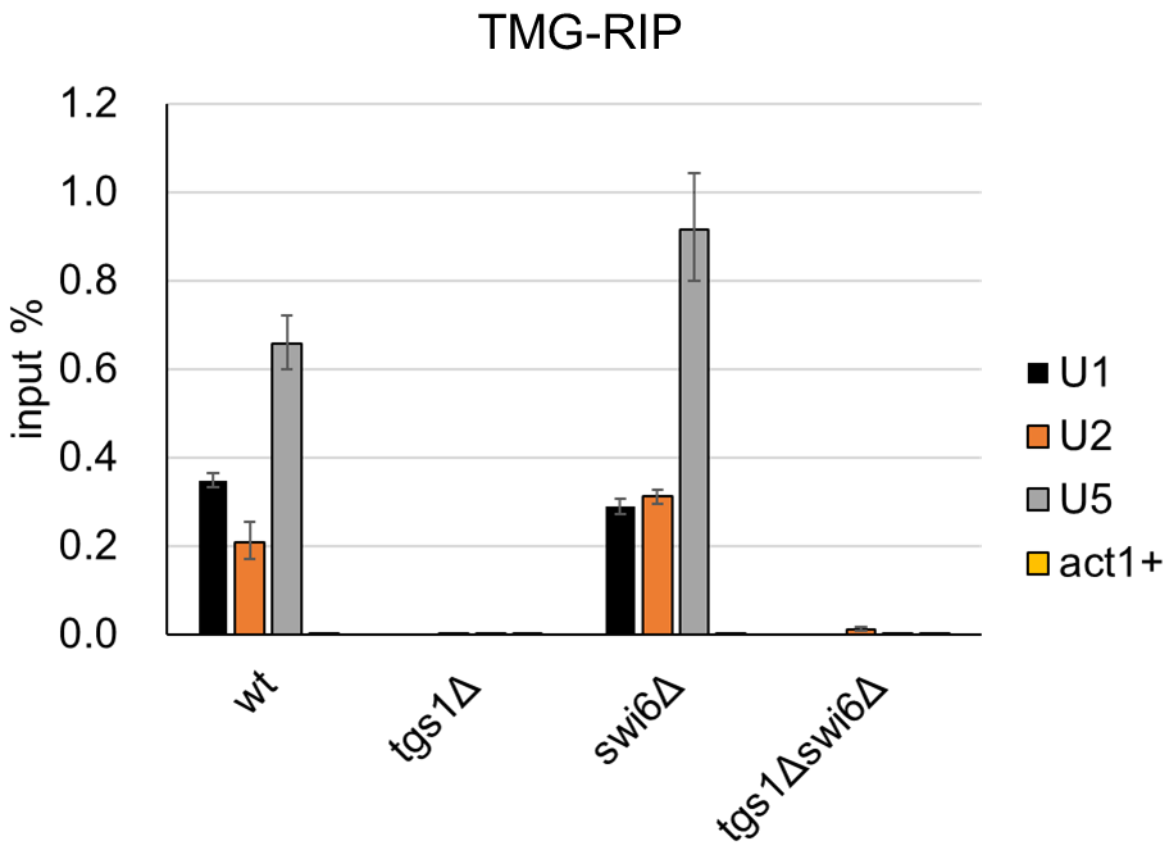

Figure 5-1 Loss of Tgs1 decreases splicing efficiency of introns of some mRNAs and hncRNAs.

RNAs harboring TMG caps were immunoprecipitated using a TMG cap-specific antibody, and precipitated RNAs were analyzed by qRT-PCR using primers specific for *U1, U2, U5,* and *act1+.* Error bars indicate the SEM from three biologically independent experiments.

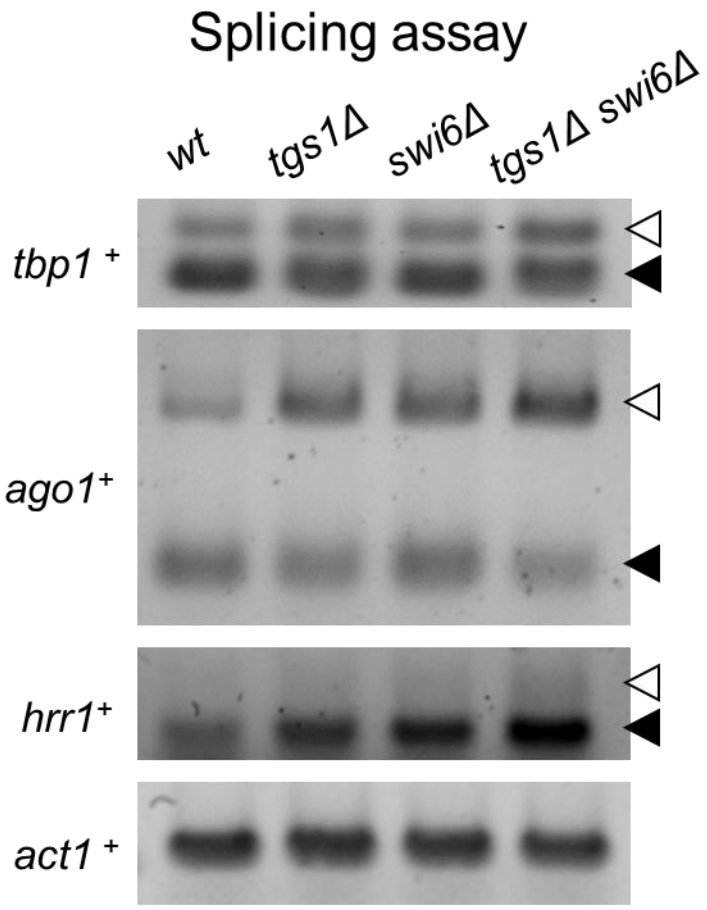

Figure 5-2 Loss of Tgs1 decreases splicing efficiency of introns of some mRNAs and hncRNAs.

Splicing efficiency analyses of mRNAs of the indicated genes were performed using primers flanking introns. The position of each primer is shown in Fig. S3. PCR products were analyzed by 1.2% agar gel. The positions of the bands that represent spliced and unspliced forms are indicated by black and white arrowheads, respectively. *act1+* was amplified as an internal control.

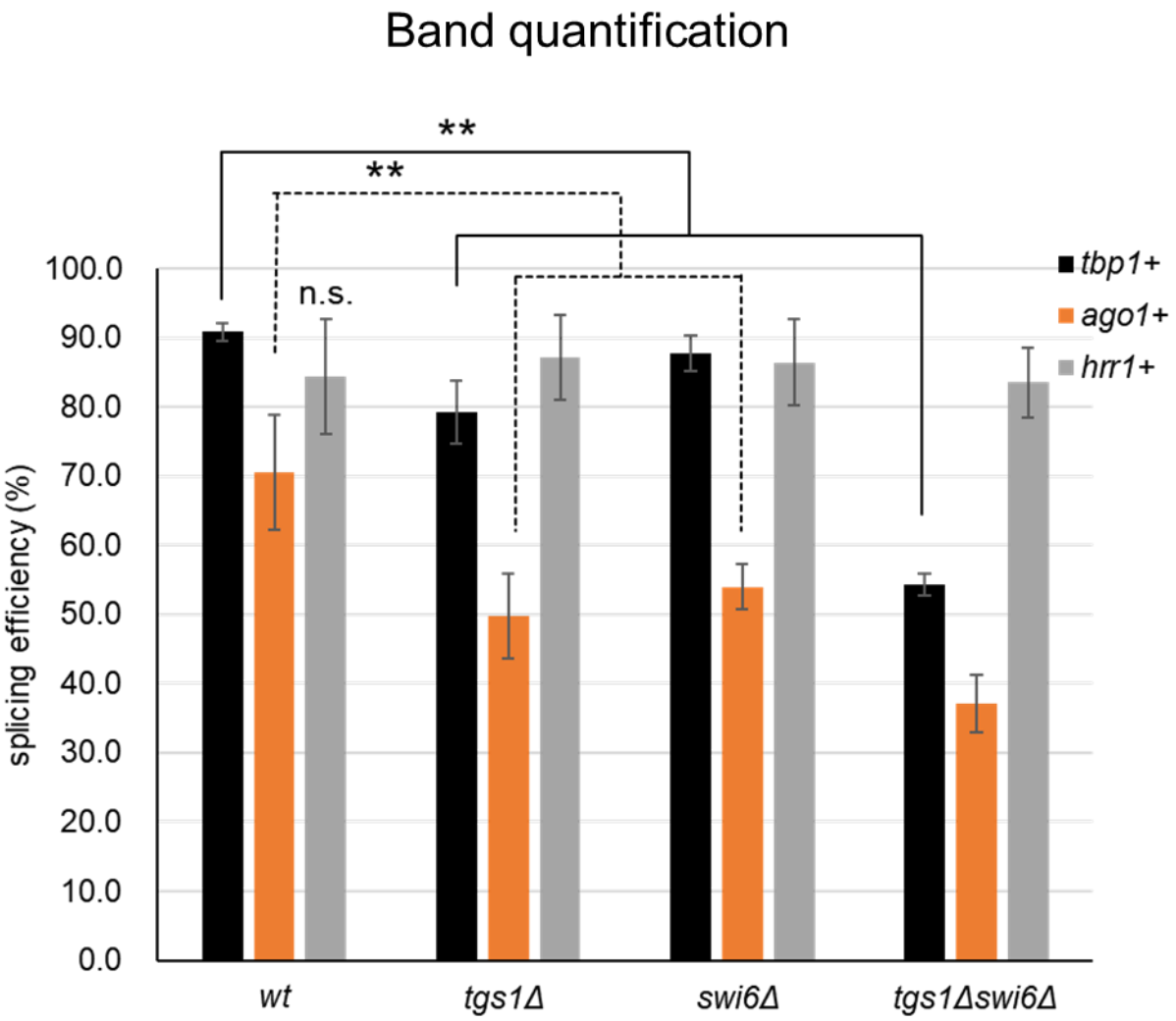

Figure 5-3 Loss of Tgs1 decreases splicing efficiency of introns of mRNAs and hncRNAs.

The intensity of bands corresponding to spliced and unspliced form in (Fig. 5-2) was quantified for 3 independent experiments using BIO RAD molecular Imager Gel Doc XR+ with Image LabTM software. Splicing efficiency of each gene was calculated by dividing amount of spliced form by total amount of spliced and unspliced form. Error bars indicate the SEM from three biologically independent experiments. **p < 0.05. p-values were determined using a two-tailed Student's t-test comparing between *wild type* and the mutants indicated by lines.

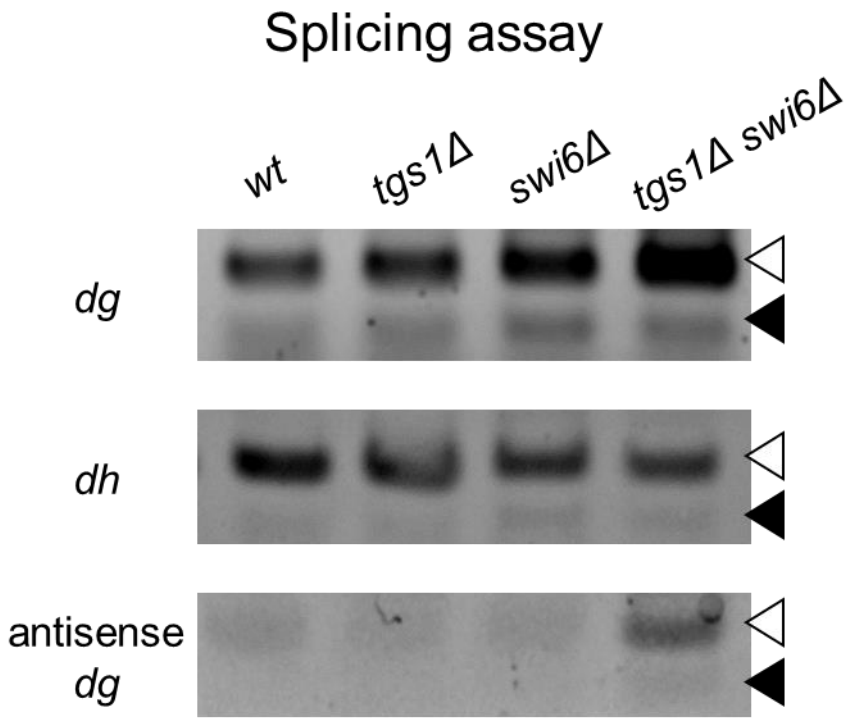

Figure 5-4 Loss of Tgs1 decreases splicing efficiency of introns of some mRNAs and hncRNAs.

Splicing efficiency analyses of mRNAs of the indicated genes were performed using primers flanking introns. The position of each primer is shown in Fig. S3. PCR products were analyzed by 1.2% agar gel. The positions of the bands that represent spliced and unspliced forms are indicated by black and white arrowheads, respectively. *act1+* was amplified as an internal control.

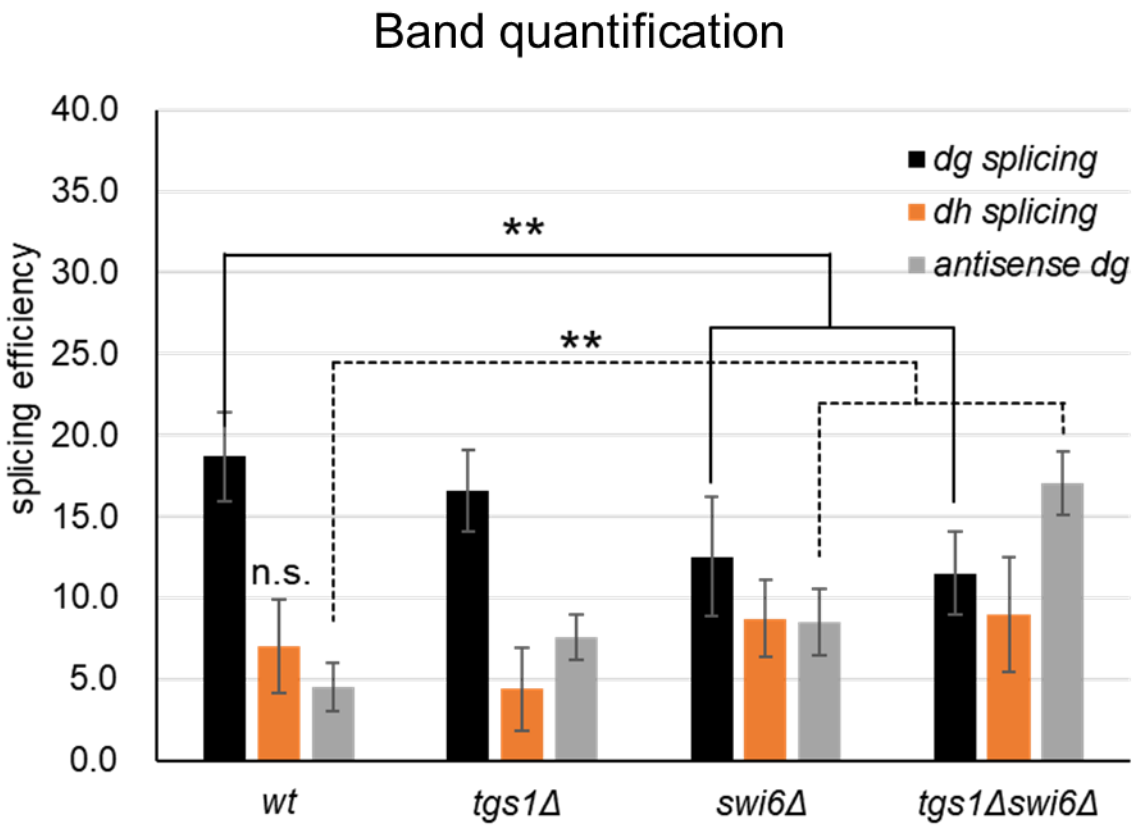

Figure 5-5 Loss of Tgs1 decreases splicing efficiency of introns of mRNAs and hncRNAs.

The intensity of bands corresponding to spliced and unspliced form in (Fig. 5-4) was quantified for 3 independent experiments using BIO RAD molecular Imager Gel Doc XR+ with Image LabTM software. Splicing efficiency of each gene was calculated by dividing amount of spliced form by total amount of spliced and unspliced form. Error bars indicate the SEM from three biologically independent experiments. **p < 0.05. p-values were determined using a two-tailed Student's t-test comparing between *wild type* and the mutants indicated by lines.

6 Tgs1 dependent TMG cap involves in retention of dg antisense transcripts on chromatin

6.1. Introduction

In addition to the RNAi factors and splicing factors mentioned in the previous chapter, there are other factors contribute to RNAi-dependent heterochromatin formation. For example, RNA polymerase II plays an active role in the production of siRNAs [19], [67]. Another important factor is the retention of heterochromatic ncRNA on chromatin, which provides a scaffold for RNAi assembly (Fig. 1-3). Previous studies in my laboratory have reported that the level of hncRNA retention on chromatin corelates with heterochromatin formation in heterochromatin mutants [19], [68], though the precious mechanism for retention is still unclear.

Interestingly, TMG cap modification by tgs1 has been reported in telomere-derived noncoding transcripts and Tgs1-dependent TMG cap is important for the maturation of telomeric RNA by the spliceosome, although the presence of cryptic intron has not been reported.

Therefore, I analyzed if heterochromatic ncRNAs have TMG cap modification and effect of the loss of Tgs1 on chromatin retention of heterochromatic ncRNA.

6.2. Experimental procedure

6.2.1. RNA immunoprecipitation for Trimethyl guanosine cap

RNA immunoprecipitation for trimethyl guanosine cap was performed as previously described in 5.2. Primers used in this section are shown (Table S2).

6.2.2. RNA immunoprecipitation for histone 3

Cells were cultured to 1×10^7 cells/mL in 50 mL of liquid YES medium. Cell lysates were prepared as described above in the ChIP assay and 2 μg/sample of RNasin Plus (Promega) was added to the buffer. Immunoprecipitation was performed with the antibody against histone H3 (Abcam). Immunoprecipitated sample and input lysate were treated with 500 μg/mL proteinase K for 60 min at 45°C and reverse cross-linked for 9 h at 65°C in the TE buffer containing 2% SDS and 80 units of RNasin Plus. Immunoprecipitated RNA was isolated by twice acid-phenol extraction and isopropanol precipitation. DNA was removed by recombinant DNase I (Takara Bio) and incubated at 37°C for 60 min. cDNA was prepared by target gene-specific reverse transcription at 42°C using the reverse primer. qPCR was performed as described above and calculated by the *ΔΔ*Ct method. The RIP signal is expressed as a percentage of input. In each graph, error bars represent SEMs from multiple biological replicates (n = 3). Primers used in this section are shown (Table S2).

6.3. Results

6.3.1. *antisense dg* transcript has Tgs1 dependent TMG cap

RIP assay with TMG-specific antibodies was performed to detect the centromeric transcripts (Fig. 6-1). *act1*$^+$, which does not have TMG cap modification was used as a negative control. Comparison between wild type and tgs1*Δ* showed that antisense dg RNA was efficiently precipitated, while dg was precipitated in small amounts. In contrast, dh RNA and negative control *act1*$^+$ mRNA was not precipitated by this antibody (Fig. 6A). Since *swi6Δ* have a more actively transcribed centromeric transcript than the wild

type, I also compared swi6 disruption and *tgs1Δswi6Δ*. From the results of wild type and swi6*Δ*, the existence of Swi6 had no effect on TMG cap modification. In addition, regardless of the presence of Swi6, Tgs1 specifically modified antisense dg with TMG.

6.3.2. TMG cap involves in retention of the transcripts on chromatin

Previously, my lab reported that immunoprecipitation results with anti-histone H3 antibodies reflect the RNAs present on heterochromatin [68], [69]. Therefore, I performed RIP with H3 antibodies and investigated how TMG cap modification contributes to chromatin localization of hncRNAs (Fig. 6-2). *Antisense dg* transcripts and small amounts of *dg* and *dh* transcripts were immunoprecipitated with histone H3. Negative control *act1*$^{+}$ was not detected. Comparison of wild-type and tgs1*Δ* showed that loss of TMG cap modification reduced the level of *antisense dg*. We also compared swi6*Δ* with *tgs1Δswi6Δ* because centromeric transcripts were actively transcribed in *swi6Δ* background. Background, the loss of TMG cap also reduced *antisense dg* levels.

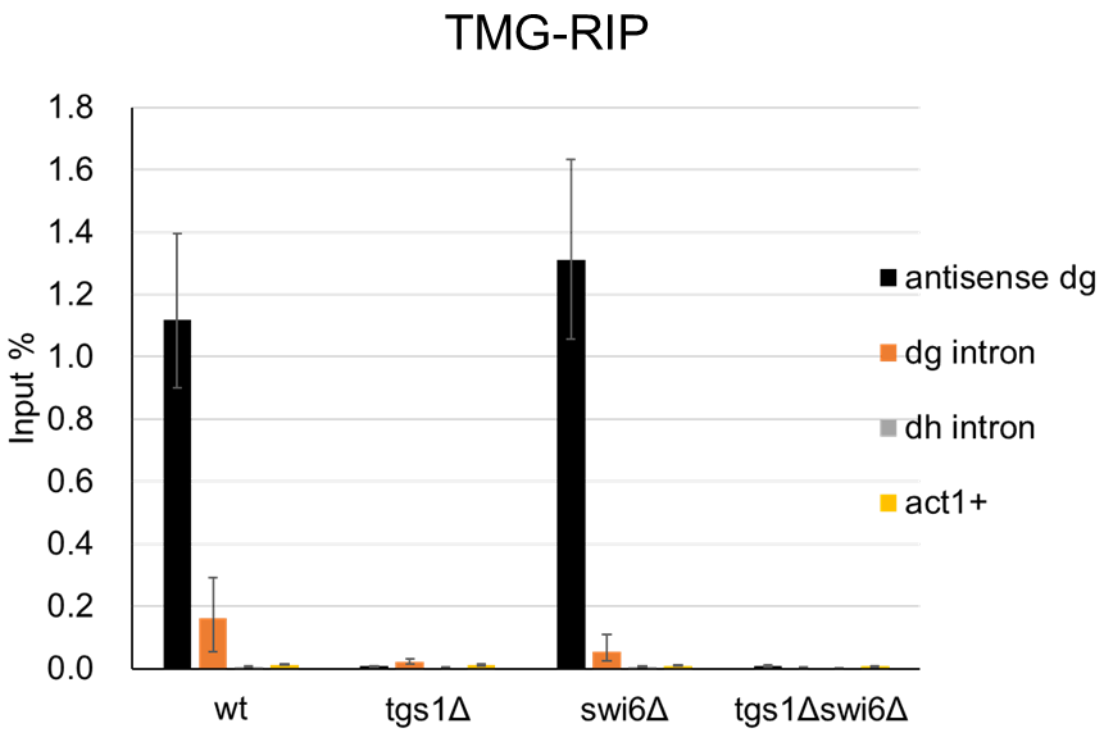

Figure 6-1 Tgs1 deletion does not affect cryptic intron splicing efficiency of heterochromatic ncRNA.

RNAs harboring TMG caps were analyzed as described in Fig. 5-1. Primer pairs for qPCR were site-specific primers for *antisense dg, dg, dh,* and *act1+*. Error bars indicate SEM from three biologically independent experiments

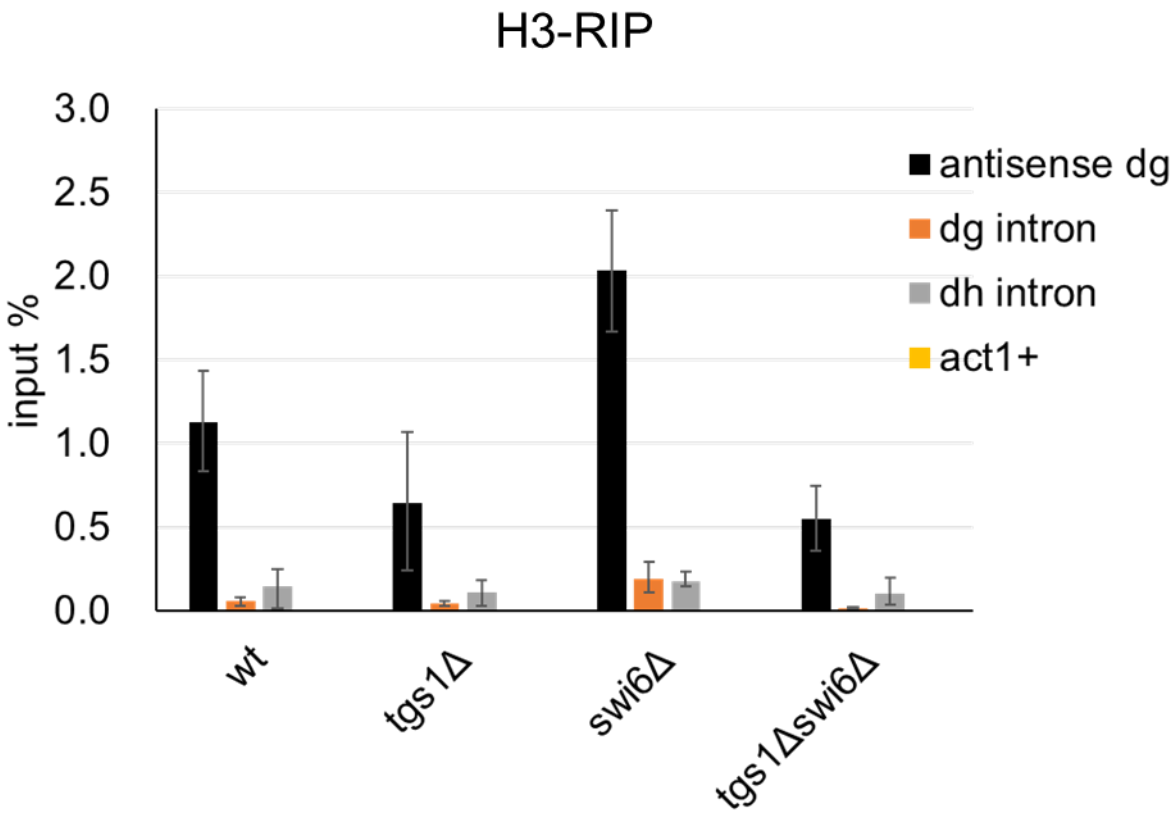

Figure 6-2 Tgs1 deletion does not affect cryptic intron splicing efficiency of heterochromatic ncRNA.

Histone H3 was immunoprecipitated, and associated RNAs were analyzed by qRT-PCR using the same primers as in (Fig. 6-1). Error bars indicate SEM from three biologically independent experiments. **$p < 0.05$. p-values were determined using a two-tailed Student's t-test comparing between wt and the mutants indicated by lines.

7 Discussion

Tgs1 is responsible for TMG capping of snRNAs and snoRNAs in eukaryotic cells. Loss of Tgs1 does not affect viability, and its precise role in the cell is not clear. In this study, I showed that loss of Tgs1 destabilizes heterochromatin. Because a mutation in a conserved amino acid in the catalytic domain of Tgs1 had the same phenotype as the deletion mutant, I concluded that the TMG cap plays a role in heterochromatin formation. Importantly, Tgs1 was required for siRNA synthesis in the absence of Swi6, although the loss of Tgs1 only marginally affected siRNA synthesis in the presence of Swi6. This suggests that the TMG cap plays a role parallel to that of Swi6 in siRNA production. RNAi factors assemble on heterochromatin and hncRNA to produce siRNA (Fig. 7-2). Swi6 recruits RDRC via a Swi6-binding protein, Ers1, which interacts with one subunit of RDRC, Hrr1, and this recruitment is important for efficient siRNA synthesis [70]. A considerable amount of siRNA, however, was still synthesized in *swi6Δ* cells, suggesting that some other mechanism recruits RDRC to heterochromatin or hncRNA. Some splicing mutants cause defects in RNAi-dependent heterochromatin formation [62], [71], and RDRC interacts with spliceosome proteins [64], [71], [72]. Because heterochromatic ncRNAs harbor introns with low splicing efficiency [64], [73], spliceosomes or sub-spliceosomes formed on hncRNA introns may recruit RDRC to hncRNA [64].

The Tgs1-dependent TMG capping of snRNA is implicated in splicing. In budding yeast, loss of Tgs1 causes a growth defect at cold temperatures and a splicing defect in some meiotic genes [58], [59]. Smaller introns and those with weaker splice sites are preferentially retained in TGS1 mutants in *melanogaster*[60]. I found that the splicing efficiencies of the introns of *tbp1*$^+$ and *ago1*$^+$ were reduced in *tgs1Δ* cells (Fig. 5-2, 3),

suggesting that the TMG cap also contributes to efficient splicing of some introns in fission yeast. Importantly, splicing efficiencies of dg and *antisense dg* cryptic introns decreased and increased in *tgs1Δswi6Δ* cells, respectively, whereas the splicing efficiency of hncRNA introns was only marginally affected in *tgs1Δ* single mutants (Fig. 5-4, 5). Therefore, the TMG cap may stabilize spliceosomes on hncRNA introns, and structural changes in the spliceosome due to loss of the TMG cap may decrease interactions between spliceosomes and RDRC. In budding yeast, analysis of spliceosome components in *tgs1Δ* cells revealed a stoichiometric association between the nuclear cap-binding protein (CBP), which binds to the MMG cap, and U1 snRNPs; the ectopic binding of CBP underlies the cold sensitive phenotype of *tgs1Δ* cells [74]. This raises the possibility that in fission yeast, ectopic binding of CBP exposes the MMG cap of snRNA in *tgs1Δ* cells, preventing the association between the spliceosome and RDRC (Fig. 7-1).

Heterochromatin assembly defects induced by splicing mutants are partially rescued by the introduction of cDNA versions of intron-containing RNAi factors such as Ago1 and Ers1 [75], indicating that the depletion of intron-containing RNAi factors by splicing defects is responsible for the heterochromatin defect. However, mutation of the dg sense intron or replacement of the intron with other euchromatic introns disrupts heterochromatin formation activity [64], indicating that the splicing process is directly involved in RNAi-dependent heterochromatin formation. Although it is possible that *tgs1Δ* indirectly affects RNAi-dependent heterochromatin by decreasing the abundance of RNAi factors encoded by intron-containing mRNAs, the level of siRNA in *tgs1Δ* cells was comparable to that in wild-type cells, implying that the indirect effect is small (Fig. 4-2).

The *clr4* deletion/reintroduction experiments showed that Tgs1 is required for efficient establishment of heterochromatin. Establishment of constitutive heterochromatin also requires the RNAi machinery [55], [76], [77], suggesting that the assembly of RNAi factors at the target loci is critical for this process. At the initial step of establishment, a small RNA called priRNA is generated from hncRNA by a cooperative function of Argonaute (Ago1) and Triman (Tri1). priRNA is essential for establishment, suggesting that it guides the RITS complex to nascent hncRNA [78]. In addition, small RNAs are produced independently on RDRC from a highly conserved sequence in antisense dg RNA called ReveCen through digestion of partially double-stranded RNA by Dcr1, and these RNAs may trigger de novo heterochromatin formation [79]. Although these RDRC-independent small RNAs can trigger heterochromatin formation, RDRC is required for the establishment of heterochromatin [76], probably by providing a stable supply of siRNA. Because the interaction of RDRC with the RITS complex depends on Clr4 and Dcr1, and the Swi6–Ers1–Hrr1 interaction is required for stable association of RDRC with heterochromatin [70], spliceosome-dependent RDRC recruitment could play a major role in assembly of RNAi factors on heterochromatin before deposition of H3K9me followed by Swi6 binding. Thus, the destabilization of the spliceosome–RDRC interaction by the loss of the TMG cap of snRNA would impair this process (Fig. 7-2).

I found that antisense dg and dg RNA harbor TMG caps. A previous study in fission yeast showed that the TMG cap of the telomerase RNA subunit, TER1, also has a TMG cap, which is required for efficient processing of telomere RNA by spliceosome [45]. Therefore, it is possible that the TMG caps of dg and antisense dg RNA contribute to the splicing of their own introns (Fig. 7-1). In addition, I found that the loss of Tgs1 decreased

the chromatin binding of these TMG-capped hncRNAs. This observation raises the possibility that the TMG cap contributes to the chromatin association of these hncRNA, providing a platform for the assembly of RNAi factors (Fig. 7-2). The possible mechanisms of Tgs1-mediated TMG cap in heterochromatin establishment described above [Fig. 7-1] are not mutually exclusive. Furthermore, it is possible that the TMG cap has other, as-yet-unknown functions.

Tgs1 and the TMG cap are required for Swi6-independent siRNA generation and establishment of heterochromatin, but only a small proportion of *tgs1Δ* cells exhibit defects in heterochromatin. Once heterochromatin is established, Swi6 assembles RNAi factors on heterochromatin, forming a stable self-enforcing loop (Fig. 7-2). Thus, TMG cap-dependent assembly of RNAi factors may play only a minor role in established heterochromatin. In some cells, however, this stable heterochromatin could be disrupted. For example, during the passage of the replication fork in heterochromatin, the temporary release of Swi6 should occur. In most cells, Swi6 would quickly re-bind to H3K9me of old nucleosomes distributed to daughter DNA and recruit RNAi factors to achieve stable heterochromatin maintenance. However, a small subset of cells in which Swi6 rebinding is delayed might require spliceosome-dependent recruitment of RNAi factors or efficient retention of hncRNA on chromatin to reestablish stable heterochromatin via RNAi.

I found that the loss of Swi6 reduced the splicing efficiencies of the euchromatic genes, $tbp1^{+}$ and $ago1^{+}$. At this stage, I did not know how Swi6, a heterochromatic protein, was involved in splicing of euchromatic genes. Because Swi6 binds to RNA nonspecifically using its hinge-domain and RNA binding is incompatible with heterochromatin association [80], this raises the possibility that Swi6 released from heterochromatin

targets to euchromatic RNA and regulates the splicing through interaction with other splicing-related proteins.

The Tgs1-dependent TMG cap system is highly conserved among eukaryotic cells, but its roles remain obscure, particularly in the nucleus. In mammalian cells, Tgs1-dependent hypermethylation of the MMG cap of snRNA and snoRNA occurs in the cytoplasm and may be required for the transport of these RNAs into the nucleus [81]. However, a recent study in *melanogaster* showed that Tgs1 mainly localizes in the nucleus, and that loss of Tgs1 does not affect the nuclear localization of snRNAs but instead causes lethality during development [60]. Therefore, based on our observations in fission yeast, I speculate that the Tgs1/TMG cap exerts its nuclear functions by controlling the activities of ncRNAs.

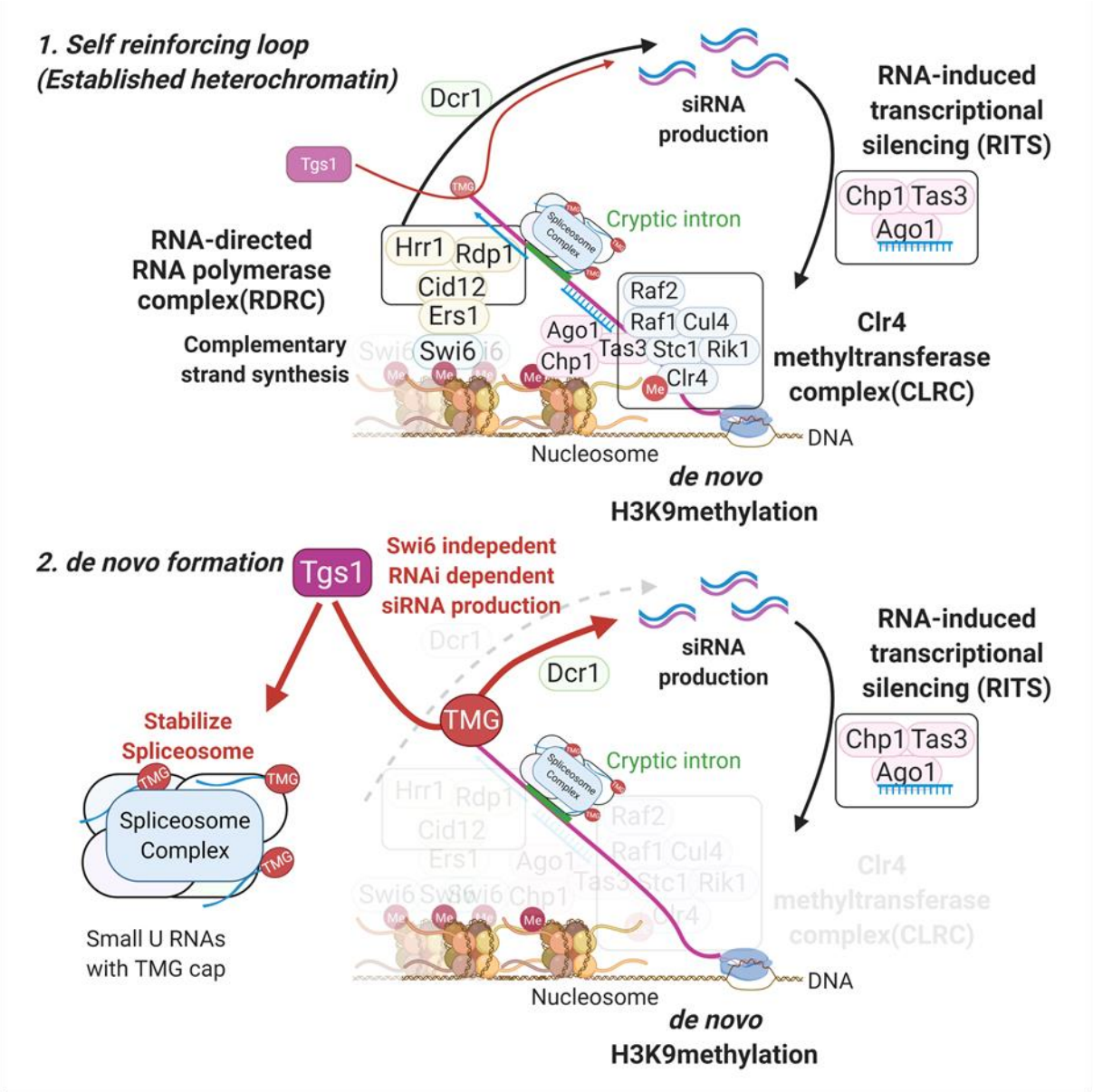

Figure 7-2 Model of function of Tgs1-mediated TMG cap in heterochromatin formation.

Tgs1 mediated TMG cap modification contributing to proper RNAi factor splicing. TMG cap could also contribute cryptic intron containing *antisense dg* RNA to assembly of spliceosomes on cryptic introns of these RNAs. Also, TMG cap modification may contribute to chromatin retention of these hncRNAs, which provides a platform of RNAi factors.

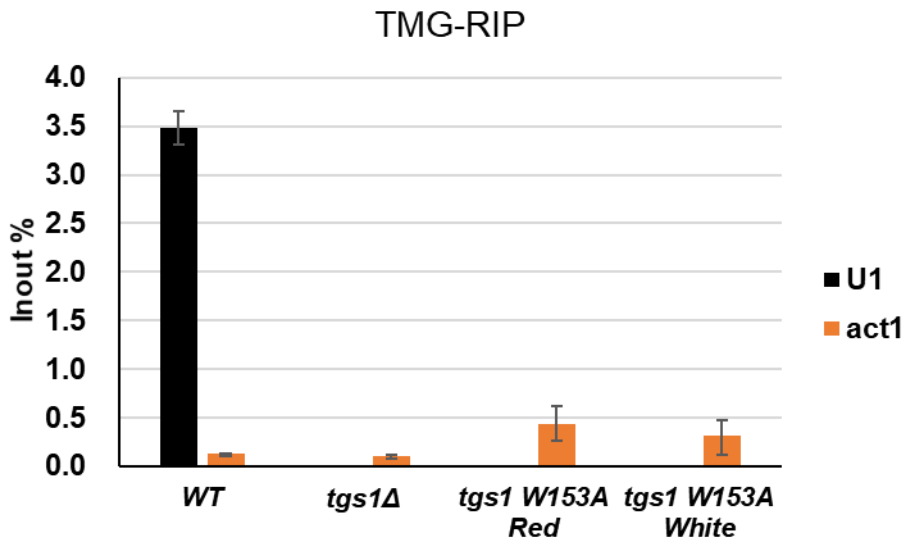

Fig.S1 TMG-RIP of Catalytically inactive mutant tgs1 W153A

RNAs harboring TMG caps were analyzed as described in Fig. 5-1. Primer pairs for qPCR were site-specific primers for *U1* and *act1*+. Error bars indicate SEM from three biologically independent experiments.

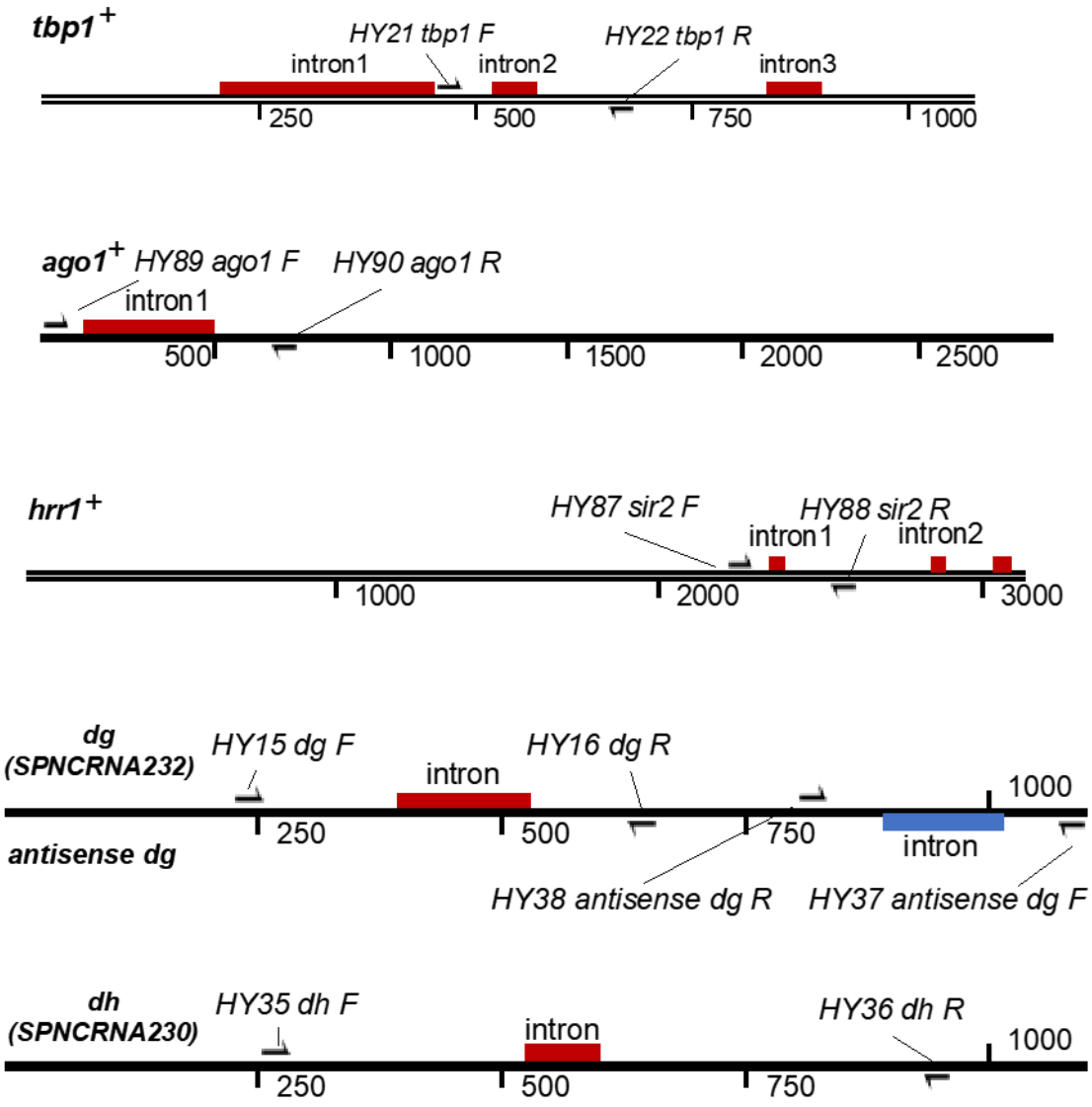

Fig. S2 The positions of primers and introns used to analyze splicing.

Table S1. List of strains used in this study

Abbreviation	Genotype	Origin
WT	*h+ ade6-DN/N leu-32 ura4-DS/E imr1L::ura4+ otr1R::ade6+*	RC Allshire[1]
Clr4Δ	*h+ ade6-DN/N leu-32 ura4-DS/E imr1L::ura4+ otr1R::ade6+ ΔClr4::KanMX6*	This work
Swi6Δ	*h+ ade6-DN/N leu-32 ura4-DS/E imr1L::ura4+ otr1R::ade6+ ΔSwi6::hphMX6*	This work
Tgs1W153A-myc-Red	*h+ ade6-DN/N leu-32 ura4-DS/E imr1L::ura4+ otr1R::ade6+ tgs1W153A-13myc-hphMX6*	This work
Tgs1W153A-myc-White	*h+ ade6-DN/N leu-32 ura4-DS/E imr1L::ura4+ otr1R::ade6+ tgs1W153A-13myc-hphMX6*	This work
Tgs1Δ	*h+ ade6-DN/N leu-32 ura4-DS/E imr1L::ura4+ otr1R::ade6+ ΔTgs1::KanMX6*	This work
tgs1-myc	*h+ ade6-DN/N leu-32 ura4-DS/E imr1L::ura4+ otr1R::ade6+ tgs1-13myc-hphMX6*	This work
Tgs1ΔClr4Δ	*h+ ade6-DN/N leu-32 ura4-DS/E imr1L::ura4+ otr1R::ade6+ ΔTgs1::KanMX6 ΔClr4::natMX6*	This work
Dcr1Δ	*h+ ade6-DN/N leu-32 ura4-DS/E imr1L::ura4+ otr1R::ade6+ ΔDcr1::KanMX6*	This work
Tgs1ΔDcr1Δ	*h+ ade6-DN/N leu-32 ura4-DS/E imr1L::ura4+ otr1R::ade6+ ΔDcr1::KanMX6 ΔTgs1::natMX6*	This work
Clr4ΔClr4(Re)	*h+ ade6-DN/N leu-32 ura4-DS/E imr1L::ura4+ otr1R::ade6+ clr4::hph::natMX6*	This work
Tgs1ΔSwi6Δ	*h+ ade6-DN/N leu-32 ura4-DS/E imr1L::ura4+ otr1R::ade6+ ΔSwi6::hph ΔTgs1::natMX6*	This work
Tgs1ΔClr4ΔClr4(Re)	*h+ ade6-DN/N leu-32 ura4-DS/E imr1L::ura4+ otr1R::ade6+ ΔTgs1::KanMX6 clr4::hph::natMX6*	This work
Tgs1Δ Red	*h+ ade6-DN/N leu-32 ura4-DS/E imr1L::ura4+ otr1R::ade6+ ΔTgs1::KanMX6*	This work
Tgs1Δ White	*h+ ade6-DN/N leu-32 ura4-DS/E imr1L::ura4+ otr1R::ade6+ ΔTgs1::KanMX6*	This work
Swi6ΔDcr1Δ	*h+ ade6-DN/N,leu1-32,ura4-DS/E,imr1L::ura4+,otr1R::ade6+,Δswi6::hphMX6Δdcr1::kanMX6*	This work

Table S2 Primers used in this study

Label	Name	Sequence	Usage
HY21	tbp1_F	CTATTGCGCTACATGCAC	Splicing defect
HY22	tbp1_R	GTCATCCTCGGATTTGCC	Splicing defect
HY33	dg(intron)_F	TCCATCCGCAGTTGGGAG	qRT-PCR or qPCR
HY34	dg(intron)_R	TACCATGCTTTTAGTGCGG	qRT-PCR or qPCR
HY35	dh(intron)_F	ACATGGCTTAGTTTCACAC	qRT-PCR or qPCR
HY36	dh(intron)_R	GCTCGACATTGTTGTTTTG	qRT-PCR or qPCR
HY37	antis. dg intron_F	ACTGCTTATCTTTTGCAACC	qRT-PCR or qPCR
HY38	antis. dg intron_R	CTCTTGTGCTCAGGCTGG	qRT-PCR or qPCR
HY43	ade6_F	TTAGTATATGCCCCTGCTCG	qRT-PCR or qPCR
HY44	ade6_R	AAATGGTCTCACCATCTTGC	qRT-PCR or qPCR
HY55	act1_F	CCCCAAATCCAACCGTGAGA	qRT-PCR or qPCR
HY56	act1_R	ATTTCACGTTCGGCGGTAGT	qRT-PCR or qPCR
HY69	snu1 F	GTCTTGGCATTGCACTGAGC	qRT-PCR or qPCR
HY70	snu1 R	CCCCAAATGAGGGACGAACT	qRT-PCR or qPCR
HY71	snu2 F	TCGCTGAAATCACCTCACTG	qRT-PCR or qPCR
HY72	snu2 R	TCGGAAAGCATAGCAAGCCA	qRT-PCR or qPCR
HY75	snu5 F	AAGCACTTTGCAAAAGCTAACG	qRT-PCR or qPCR
HY76	snu5 R	AGCACACCTTACAAACGGCT	qRT-PCR or qPCR
HY85	Hrr1 F	GGAATATACTCGGTTGAC	Splicing defect
HY86	Hrr1 R	CTAACATCTGAGCTTCG	Splicing defect
HY89	ago1 F	CCTAACGAGACTATCAAC	Splicing defect
HY90	ago1 R	CTTGATGGTGCCATCAGC	Splicing defect
AG-380	cen-dh Fw	TTCTCAACCTTCCGACGC	Northern blot analysis of siRNA
AG-381	cen-dh Rv	CTGTCATCCAAGTGGAATG	Northern blot analysis of siRNA
AG-382	cen-dg Fw	CACCACTTCCACTTACCACTTCC	Northern blot analysis of siRNA
AG-383	cen-dg Rv	ACAGGATCATCGAGAAGAGTAG	Northern blot analysis of siRNA
AG-384	snoRNA58	GATGAAATTCAGAAGTCTAGCATC	Northern blot analysis of siRNA

8 Reference

[1] C. P. Ponting, P. L. Oliver, and W. Reik, “Evolution and Functions of Long Noncoding RNAs,” *Cell*, vol. 136, no. 4, pp. 629–641, 2009.

[2] A. G. West, S. Huang, M. Gaszner, M. D. Litt, and G. Felsenfeld, “Recruitment of histone modifications by USF proteins at a vertebrate barrier element,” *Mol. Cell*, vol. 16, no. 3, pp. 453–463, 2004.

[3] M. Iizuka and M. M. Smith, “Functional consequences of histone modifications,” *Curr. Opin. Genet. Dev.*, vol. 13, no. 2, pp. 154–160, 2003.

[4] C. Yan and D. D. Boyd, “Histone H3 Acetylation and H3 K4 Methylation Define Distinct Chromatin Regions Permissive for Transgene Expression,” *Mol. Cell. Biol.*, vol. 26, no. 17, pp. 6357–6371, 2006.

[5] R. C. Allshire, J. P. Javerzat, N. J. Redhead, and G. Cranston, “Position effect variegation at fission yeast centromeres,” *Cell*, vol. 76, no. 1, pp. 157–169, 1994.

[6] K. L. Huisinga, B. Brower-Toland, and S. C. R. Elgin, “The contradictory definitions of heterochromatin: Transcription and silencing,” *Chromosoma*, vol. 115, no. 2, pp. 110–122, 2006.

[7] R. C. Allshire and K. Ekwall, “Epigenetic regulation of chromatin states in Schizosaccharomyces pombe,” *Cold Spring Harb. Perspect. Biol.*, vol. 7, no. 7, pp. 1–25, 2015.

[8] M. Sorida *et al.*, “Regulation of ectopic heterochromatin-mediated epigenetic diversification by the JmjC family protein Epe1,” *PLoS Genet.*, vol. 15, no. 6, pp. 1–29, 2019.

[9] S. Guang, A. F. Bochner, K. B. Burkhart, N. Burton, D. M. Pavelec, and S. Kennedy, “Small regulatory RNAs inhibit RNA polymerase II during the elongation phase of transcription,” *Nature*, vol. 465, no. 7301, pp. 1097–1101, 2010.

[10] J. Y. Parsa, S. Boudoukha, J. Burke, C. Homer, and H. D. Madhani, “Polymerase pausing induced by sequence-specific RNA-binding protein drives heterochromatin assembly,” *Genes Dev.*, vol. 32, no. 13–14, pp. 953–964, 2018.

[11] Y. Shimada, F. Mohn, and M. Bühler, “The RNA-induced transcriptional silencing complex targets chromatin exclusively via interacting with nascent transcripts,” *Genes Dev.*, vol. 30, no. 23, pp. 2571–2580, 2016.

[12] Y. Chikashige *et al.*, “Composite motifs and repeat symmetry in S. pombe centromeres: Direct analysis by integration of NotI restriction sites,” *Cell*, vol. 57, no. 5, pp. 739–751, 1989.

[13] S. Murakami, M. Yanagida, and O. Niwa, “A large circular minichromosome of Schizosaccharomyces pombe requires a high dose of type II DNA topoisomerase for its stabilization,” *MGG Mol. Gen. Genet.*, vol. 246, no. 6, pp. 671–679, 1995.

[14] K. Ekwall, “The roles of histone modifications and small RNA in centromere function,” *Chromosom. Res.*, vol. 12, no. 6, pp. 535–542, 2004.

[15] A. Smialowska, I. Djupedal, J. Wang, P. Kylsten, P. Swoboda, and K. Ekwall, “RNAi mediates post-transcriptional repression of gene expression in fission yeast Schizosaccharomyces pombe,” *Biochem. Biophys. Res. Commun.*, vol. 444, no. 2, pp. 254–259, 2014.

[16] K. R. Hansen, P. T. Ibarra, and G. Thon, “Evolutionary-conserved telomere-linked helicase genes of fission yeast are repressed by silencing factors, RNAi components and the telomere-binding protein Taz1,” *Nucleic Acids Res.*, vol. 34, no. 1, pp. 78–88, 2006.

[17] T. Sugiyama, H. Cam, A. Verdel, D. Moazed, and S. I. S. Grewal, “RNA-dependent RNA polymerase is an essential component of a self-enforcing loop coupling heterochromatin assembly to siRNA production,” *Proc. Natl. Acad. Sci. U. S. A.*, vol. 102, no. 1, pp. 152–157, 2005.

[18] H. Kato and Y. Murakami, “Heterochromatin and centromere: heterochromatin meets RNAi,” *Tanpakushitsu Kakusan Koso.*, vol. 49, no. 12, pp. 1990–1997, 2004.

[19] T. Kajitani *et al.*, “Ser7 of RNAPII-CTD facilitates heterochromatin formation by linking ncRNA to RNAi,” *Proc. Natl. Acad. Sci.*, p. 201714579, 2017.

[20] T. Hori *et al.*, “Constitutive centromere-associated network controls centromere drift in vertebrate cells,” *J. Cell Biol.*, vol. 216, no. 1, pp. 101–113, 2017.

[21] K. Plath, S. Mlynarczyk-Evans, D. A. Nusinow, and B. Panning, “Xist RNA and the Mechanism of X Chromosome Inactivation ,” *Annu. Rev. Genet.*, vol. 36, no. 1, pp. 233–278, 2002.

[22] J. M. Autuoro, S. P. Pirnie, and G. G. Carmichael, “Long noncoding RNAs in imprinting and X chromosome inactivation,” *Biomolecules*, vol. 4, no. 1, pp. 76–100, 2014.

[23] R. C. Allshire and K. Ekwall, “Epigenetic regulation of chromatin states in Schizosaccharomyces pombe,” *Cold Spring Harb. Perspect. Biol.*, vol. 7, no. 7, pp. 1–25, 2015.

[24] J. A. Fawcett *et al.*, “Population genomics of the fission yeast Schizosaccharomyces pombe,” *PLoS One*, vol. 9, no. 8, 2014.

[25] J. Wixon, “Featured organism: Schizosaccharomyces pombe, the fission yeast,” *Comp. Funct. Genomics*, vol. 3, no. 2, pp. 194–204, 2002.

[26] S. Hausmann and S. Shuman, “Specificity and mechanism of RNA cap guanine-N2 methyltransferase (Tgs1),” *J. Biol. Chem.*, vol. 280, no. 6, pp. 4021–4024, 2005.

[27] J. Mouaikel, C. Verheggen, E. Bertrand, J. Tazi, and R. Bordonné, “Hypermethylation of the cap structure of both yeast snRNAs and snoRNAs requires a conserved methyltransferase that is localized to the nucleolus,” *Mol. Cell*, vol. 9, no. 4, pp. 891–901, 2002.

[28] Y. Zhu, C. Qi, W. Q. Cao, A. V. Yeldandi, M. S. Rao, and J. K. Reddy, “Cloning and characterization of PIMT, a protein with a methyltransferase domain, which interacts with and enhances nuclear receptor coactivator PRIP function,” *Proc. Natl. Acad. Sci. U. S. A.*, vol. 98, no. 18, pp. 10380–10385, 2001.

[29] C. Girard *et al.*, “Characterization of a short isoform of human Tgs1 hypermethylase associating with small nucleolar ribonucleoprotein core proteins and produced by limited proteolytic processing,” *J. Biol. Chem.*, vol. 283, no. 4, pp. 2060–2069, 2008.

[30] J. peng Ruan, E. Ullu, and C. Tschudi, “Characterization of the Trypanosoma brucei cap hypermethylase Tgs1,” *Mol. Biochem. Parasitol.*, vol. 155, no. 1, pp. 66–69, 2007.

[31] I. Enünlü, G. Pápai, I. Cserpán, A. Udvardy, K. T. Jeang, and I. Boros, “Different isoforms of PRIP-interacting protein with methyltransferase domain/trimethylguanosine synthase localizes to the cytoplasm and nucleus,” *Biochem. Biophys. Res. Commun.*, vol. 309, no. 1, pp. 44–51, 2003.

[32] T. Monecke, A. Dickmanns, and R. Ficner, “Structural basis for m7G-cap hypermethylation of small nuclear, small nucleolar and telomerase RNA by the dimethyltransferase TGS1,” *Nucleic Acids Res.*, vol. 37, no. 12, pp. 3865–3877, 2009.

[33] J. Chang, B. Schwer, and S. Shuman, “Mutational analyses of trimethylguanosine synthase (Tgs1) and Mud2: Proteins implicated in pre-mRNA splicing,” *Rna*, vol. 16, no. 5, pp. 1018–1031, 2010.

[34] S. Hausmann *et al.*, “Genetic and biochemical analysis of yeast and human cap trimethylguanosine synthase: Functional overlap of 2,2,7-trimethylguanosine caps, small nuclear ribonucleoprotein components, PRE-mRNA splicing factors, and RNA decay pathways,” *J. Biol. Chem.*, vol. 283, no. 46, pp. 31706–31718, 2008.

[35] L. Chen *et al.*, “Loss of Human TGS1 Hypermethylase Promotes Increased Telomerase RNA and Telomere Elongation,” *Cell Rep.*, vol. 30, no. 5, pp. 1358-1372.e5, 2020.

[36] V. S. R. K. Yedavalli and K. T. Jeang, “Rev-ing up post-transcriptional HIV-1 RNA expression,” *RNA Biol.*, vol. 8, no. 2, 2011.

[37] M. Jankowska-Anyszka, K. Piecyk, and J. Šamonina-Kosicka, “Synthesis of a new class of ribose functionalized dinucleotide cap analogues for biophysical studies on interaction of cap-binding proteins with the 5′ end of mRNA,” *Org. Biomol. Chem.*, vol. 9, no. 15, pp. 5564–5572, 2011.

[38] A. Mourão, A. Varrot, C. D. Mackereth, S. Cusack, and M. Sattler, “Structure and RNA recognition by the snRNA and snoRNA transport factor PHAX,” *Rna*, vol. 16, no. 6, pp. 1205–1216, 2010.

[39] D. Becker, A. G. Hirsch, L. Bender, T. Lingner, G. Salinas, and H. Krebber, “Nuclear Pre-snRNA Export Is an Essential Quality Assurance Mechanism for Functional Spliceosomes,” *Cell Rep.*, vol. 27, no. 11, pp. 3199-3214.e3, 2019.

[40] A. Camasses, E. Bragado-Nilsson, R. Martin, B. Séraphin, and R. Bordonné, “Interactions within the Yeast Sm Core Complex: from Proteins to Amino Acids,” *Mol. Cell. Biol.*, vol. 18, no. 4, pp. 1956–1966, 1998.

[41] M. Morlando, P. Greco, B. Dichtl, A. Fatica, W. Keller, and I. Bozzoni, “Functional Analysis of Yeast snoRNA and snRNA 3′-End Formation Mediated by Uncoupling of Cleavage and Polyadenylation,” *Mol. Cell. Biol.*, vol. 22, no. 5, pp. 1379–1389, 2002.

[42] F. Gallardo, C. Olivier, A. T. Dandjinou, R. J. Wellinger, and P. Chartrand, “TLC1 RNA nucleo-cytoplasmic trafficking links telomerase biogenesis to its recruitment to telomeres,” *EMBO J.*, vol. 27, no. 5, pp. 748–757, 2008.

[43] E. H. Blackburn, E. S. Epel, and J. Lin, “Human telomere biology: A contributory and interactive factor in aging, disease risks, and protection,” *Science (80-.).*, vol. 350, no. 6265, pp. 1193–1198, 2015.

[44] Y. Vasianovich and R. J. Wellinger, “Life and Death of Yeast Telomerase RNA,” *J. Mol. Biol.*, vol. 429, no. 21, pp. 3242–3254, 2017.

[45] W. Tang, R. Kannan, M. Blanchette, and P. Baumann, “Telomerase RNA biogenesis involves sequential binding by Sm and Lsm complexes,” *Nature*, vol. 484, no. 7393, pp. 260–264, 2012.

[46] O. Komonyi *et al.*, “DTL, the Drosophila homolog of PIMT/Tgs1 nuclear receptor coactivator-interacting protein/RNA methyltransferase, has an essential role in development,” *J. Biol. Chem.*, vol. 280, no. 13, pp. 12397–12404, 2005.

[47] Y. Jia *et al.*, “Early embryonic lethality of mice with disrupted transcription cofactor PIMT/NCOA6IP/Tgs1 gene,” *Mech. Dev.*, vol. 129, no. 9–12, pp. 193–207, 2012.

[48] A. Matsuyama *et al.*, “ORFeome cloning and global analysis of protein localization in the fission yeast Schizosaccharomyces pombe,” *Nat. Biotechnol.*, vol. 24, no. 7, pp. 841–847, 2006.

[49] A. Shimada *et al.*, “Phosphorylation of Swi6/HP1 regulates transcriptional gene silencing at heterochromatin,” *Genes Dev.*, vol. 23, no. 1, pp. 18–23, 2009.

[50] P. Schuchert and J. Kohli, “The Ade6-M26 Mutation of Schizosaccharomyces Pombe Increases the Frequency of Crossing over.,” *Genetics*, vol. 119, no. 3, pp. 507–50715, 1988.

[51] J. B. Keeney and J. D. Boeke, “Efficient targeted integration at leu1-32 and ura4-294 in Schizosaccharomyces pombe,” *Genetics*, vol. 136, no. 3, pp. 849–856, 1994.

[52] Q. Geissmann, “OpenCFU, a New Free and Open-Source Software to Count Cell Colonies and Other Circular Objects,” *PLoS One*, vol. 8, no. 2, pp. 1–10, 2013.

[53] S. Schneider, B. Schwer, S. Shuman, A. Ramirez, and S. Hausmann, “Biochemical and genetic analysis of RNA cap guanine-N2 methyltransferases from Giardia lamblia and Schizosaccharomyces pombe,” *Nucleic Acids Res.*, vol. 35, no. 5, pp. 1411–1420, 2007.

[54] S. Hausmann, A. Ramirez, S. Schneider, B. Schwer, and S. Shuman, “Biochemical and genetic analysis of RNA cap guanine-N2 methyltransferases from Giardia lamblia and Schizosaccharomyces pombe,” *Nucleic Acids Res.*, vol. 35, no. 5, pp. 1411–1420, 2007.

[55] M. Sadaie, T. Iida, T. Urano, and J. I. Nakayama, “A chromodomain protein, Chp1, is required for the establishment of heterochromatin in fission yeast,” *EMBO J.*, vol. 23, no. 19, pp. 3825–3835, 2004.

[56] M. Sadaie, T. Iida, T. Urano, and J. I. Nakayama, “A chromodomain protein, Chp1, is required for the establishment of heterochromatin in fission yeast,” *EMBO J.*, vol. 23, no. 19, pp. 3825–3835, 2004.

[57] A. Buscaino, E. Lejeune, P. Audergon, G. Hamilton, A. Pidoux, and R. C. Allshire, “Distinct roles for Sir2 and RNAi in centromeric heterochromatin nucleation, spreading and maintenance,” *EMBO J.*, vol. 32, no. 9, pp. 1250–1264, 2013.

[58] J. Mouaikel, C. Verheggen, E. Bertrand, J. Tazi, and R. Bordonné, “Hypermethylation of the cap structure of both yeast snRNAs and snoRNAs requires a

conserved methyltransferase that is localized to the nucleolus," *Mol. Cell*, vol. 9, no. 4, pp. 891–901, 2002.

[59] Z. R. Qiu, S. Shuman, and B. Schwer, "An essential role for trimethylguanosine RNA caps in Saccharomyces cerevisiae meiosis and their requirement for splicing of SAE3 and PCH2 meiotic pre-mRNAs," *Nucleic Acids Res.*, vol. 39, no. 13, pp. 5633–5646, 2011.

[60] L. Cheng, Y. Zhang, Y. Zhang, T. Chen, Y. Z. Xu, and Y. S. Rong, "Loss of the RNA trimethylguanosine cap is compatible with nuclear accumulation of spliceosomal snRNAs but not pre-mRNA splicing or snRNA processing during animal development," *PLoS Genet.*, vol. 16, no. 10, pp. 1–28, 2020.

[61] E. H. Bayne *et al.*, "Splicing factors facilitate RNAi-directed silencing in fission yeast," *Science (80-.).*, vol. 322, no. 5901, pp. 602–606, 2008.

[62] M. Chinen, M. Morita, K. Fukumura, and T. Tani, "Involvement of the spliceosomal U4 small nuclear RNA in heterochromatic gene silencing at fission yeast centromeres," *J. Biol. Chem.*, vol. 285, no. 8, pp. 5630–5638, 2010.

[63] S. P. Kallgren *et al.*, "The Proper Splicing of RNAi Factors Is Critical for Pericentric Heterochromatin Assembly in Fission Yeast," *PLoS Genet.*, vol. 10, no. 5, pp. 1–11, 2014.

[64] M. Mutazono *et al.*, "The intron in centromeric noncoding RNA facilitates RNAi-mediated formation of heterochromatin," *PLoS Genet.*, vol. 13, no. 2, pp. 1–25, 2017.

[65] N. N. Lee *et al.*, “XMtr4-like protein coordinates nuclear RNA processing for heterochromatin assembly and for telomere maintenance,” *Cell*, vol. 155, no. 5, p. 1061, 2013.

[66] S. Urushiyama, T. Tani, and Y. Ohshima, “Isolation of novel pre-mRNA splicing mutants of Schizosaccharomyces pombe,” *Mol. Gen. Genet.*, vol. 253, no. 1–2, pp. 118–127, 1996.

[67] H. Kato, D. B. Goto, R. A. Martienssen, T. Urano, K. Furukawa, and Y. Murakami, “Molecular Biology: RNA polymerase II is required for RNAi-dependent heterochromatin assembly,” *Science (80-.).*, vol. 309, no. 5733, pp. 467–469, 2005.

[68] M. Nakama, K. Kawakami, T. Kajitani, T. Urano, and Y. Murakami, “DNA-RNA hybrid formation mediates RNAi-directed heterochromatin formation,” *Genes to Cells*, vol. 17, no. 3, pp. 218–233, 2012.

[69] T. Kajitani *et al.*, “Ser7 of RNAPII-CTD facilitates heterochromatin formation by linking ncRNA to RNAi,” *Proc. Natl. Acad. Sci.*, vol. 114, no. 52, pp. E11208–E11217, 2017.

[70] A. Hayashi, M. Ishida, R. Kawaguchi, T. Urano, Y. Murakami, and J. I. Nakayama, “Heterochromatin protein 1 homologue Swi6 acts in concert with Ers1 to regulate RNAi-directed heterochromatin assembly,” *Proc. Natl. Acad. Sci. U. S. A.*, vol. 109, no. 16, pp. 6159–6164, 2012.

[71] E. H. Bayne, D. A. Bijos, S. A. White, F. de Lima Alves, J. Rappsilber, and R. C. Allshire, “A systematic genetic screen identifies new factors influencing centromeric heterochromatin integrity in fission yeast,” *Genome Biol.*, vol. 15, no. 10, p. 481, 2014.

[72] D. Moazed *et al.*, “Studies on the mechanism of RNAi-dependent heterochromatin assembly,” *Cold Spring Harb. Symp. Quant. Biol.*, vol. 71, pp. 461–671, 2006.

[73] Y. J. Lee *et al.*, “RNA polymerase I stability couples cellular growth to metal availability,” *Mol. Cell*, vol. 51, no. 1, pp. 105–115, 2013.

[74] B. Schwer, H. Erdjument-Bromage, and S. Shuman, “Composition of yeast snRNPs and snoRNPs in the absence of trimethylguanosine caps reveals nuclear cap binding protein as a gained U1 component implicated in the cold-sensitivity of tgs1δ cells,” *Nucleic Acids Res.*, vol. 39, no. 15, pp. 6715–6728, 2011.

[75] A. Shetty *et al.*, “Spt5 Plays Vital Roles in the Control of Sense and Antisense Transcription Elongation,” *Mol. Cell*, vol. 66, no. 1, pp. 77-88.e5, 2017.

[76] I. M. Hall, G. D. Shankaranarayana, K. ichi Noma, N. Ayoub, A. Cohen, and S. I. S. Grewal, “Establishment and maintenance of a heterochromatin domain,” *Science (80-.).*, vol. 297, no. 5590, pp. 2232–2237, 2002.

[77] K. Ekwall, “The RITS Complex - A Direct Link between Small RNA and Heterochromatin,” *Mol. Cell*, vol. 13, no. 3, pp. 304–305, 2004.

[78] M. Marasovic, M. Zocco, and M. Halic, “Argonaute and triman generate dicer-independent prirnas and mature siRNAs to initiate heterochromatin formation,” *Mol. Cell*, vol. 52, no. 2, pp. 173–183, 2013.

[79] I. Djupedal and K. Ekwall, “Epigenetics: Heterochromatin meets RNAi,” *Cell Res.*, vol. 19, no. 3, pp. 282–295, 2009.

[80] C. Keller, R. Adaixo, R. Stunnenberg, K. J. Woolcock, S. Hiller, and M. Bühler, “HP1 Swi6 Mediates the Recognition and Destruction of Heterochromatic RNA Transcripts,” *Mol. Cell*, vol. 47, no. 2, pp. 215–227, 2012.

[81] J. Hamm and I. W. Mattaj, “Monomethylated cap structures facilitate RNA export from the nucleus,” *Cell*, vol. 63, no. 1, pp. 109–118, 1990.

9 Acknowledgements

I would like to express my deepest appreciation to my supervisor, Professor Yota Murakami for his superior guidance, and extensive discussions. I would like to thank Professor Kazuyasu Sakaguchi (Laboratory of Biological Chemistry), Professor Akinori Takaoka (Division of Signaling in Cancer and Immunology, Institute for Genetic Medicine), and Mutsumi Takagi (Laboratory of Cell Processing Engineering) for their suggestions and guidance on my papers.

I wish to express my profound gratitude to Associate Professor Masayuki Takahashi, Assistant Professor Shinya Takahata who provided helpful suggestions and encouragement. I am also very grateful to all the members of the Laboratory of Bioorganic Chemistry. I would also like to thank the ambitious leader’s program for financial support through my Ph.D. study.

Finally, I would like to extend my indebtedness to my parents for constant encouragement throughout my studies.